THE NATURE OF THE COMPACT STRUCTURE OF 3C454.3

by

Robert F. Willson

A.B Harvard College June 1974

SUBMITTED IN PARTIAL FULFILLMENT

OF THE REQUIREMENTS FOR THE

DEGREE OF

MASTER OF SCIENCE

at the

MASSACHUSETTS INSTITUTE OF TECHNOLOGY

January 21,1977

Signature of Author.....
Department of Earth and Planetary Sciences

Certified by.....
Thesis supervisor

Accepted by.....

THE NATURE OF THE COMPACT STRUCTURE OF 3C454.3

by

Robert Frederick Willson

Submitted to the Massachusetts Institute of Technology on January 26, 1977, in partial fulfillment of the requirements for the degree of Master of Science

ABSTRACT

The quasar 3C454.3 has been observed at 7.8 Ghz using very-long baseline interferometry during nine experiments extending from April 1972 to May 1974. An attempt to model the brightness distribution using correlated flux* and closure-phase data shows that the source consists of several components some of which have undergone changes in their strength during the span of the observations. These results together with total flux data at 7.8 GHz and other frequencies have been used to provide estimates for the magnetic field and energy requirements of the source.

Total flux variations have been found to be inconsistent with an outburst for which the relativistic electrons are injected instantaneoulsly. Good agreement is found for a prolonged injection model but the absence of variations at 2.7 GHz suggests that thermal absorption may be present at least in part of the source.

*We omit the modifier, sensity, throughout the paper. Flux is understood to mean flux density.

I. INTRODUCTION

One of the fundamental problems in astronomy is the understanding of the nature of variable highly energetic extragalactic radio sources. Centimeter-wavelength very-long-baseline interferometry involving antennas separated by intercontinental distances provides angular resolution on the order of $1''\times10^{-3}$ and is therefore a useful tool for probing the compact structure of these objects.

Recent VLBI studies have revealed that quasars and active galaxies exhibit a variety of structure ranging from simple to complex (eg. Wittels et al.,1975, Schilizzi et al, 1975a,b). For many sources the radio brightness distribution can be adequately represented by a "core-halo" model for which part of the total flux originates in a single unresolved or slightly resolved component while the remaining flux is contained in a larger source or "halo" with sizes up to an arc minute. Other sources are more complex and consist of a number of components with different sizes and strengths, although arranged in basically a linear manner. Moreover, the structure of several sources namely 3C120, 3C273 and 3C345 appears to change rapidly with time (Whitney et al.,1971, Cohen et al,1976,Wittels et al.,1976) and these changes have been interpreted as apparent superrelativistic expansion or separation of the individual components.

Observation of other objects are needed for a number of reasons, one being to determine whether this superrelativistic expansion phenomenon is characteristic of all multi-component

sources or is a feature of just a few. More importantly however a knowledge of the spatial dimensions, inferred by the angular size and assumed distance, with total flux, polarization, optical and x-ray data may provide information needed to understand the formation, evolution and energetics of these objects.

The radio source 3C454.3 ($\alpha = 22^h51^m29^s$, $\delta = +15^o52'54''$ (1950.0)) has been reasonably well studied during the past few years. Its optical counterpart which is coincident in position with the radio source has been identified as a quasi-stellar object on the basis of a blue, nonthermal optical continuum, stellar appearance on photographic plates and a moderately high redshift of z=.86 (Burbidge and Burbidge,1967; Lynds,1967). Assuming a cosmological origin for the redshift with H_o=55 km/sec/Mpc and q_o=.1, yields a source luminosity distance of 6.5×10^9 parsecs. At this distance one milli-arc second of angular separation corresponds to a projected linear dimension of 9.1 parsecs.

During the last ten years, the source has been monitored by many groups at radio and optical wavelengths and has exhibited intensity variations in both portions of the spectrum. Pomphrey et al. (1976) have shown however, that there exists little if any correlation between either the times or the numbers of the optical and radio outbursts.

Figure 1 shows the optical data, taken from the literature, for the period between 1967 and 1976. The light curve is characterized by a more or less constant background level, interrupted by outbursts during 1967,1968 and 1970. In each case the brightness appeared to fluctuate by about 1 magnitude

over a period of a few months, although a close examination of the data reveals that the outburst which occurred during the latter part of 1970 may have consisted of two separate flares, separated in time by about a month. Variations of $\sim$.3 magnitudes on a timescale as short as a few days have also been reported (Angione 1971a). Spectroscopic observations by Visvanathan(1973) have shown that although the optical continuum changes rapidly the emission line strengths remain constant.

We have made photographic observations of the source on four nights during October and November 1975 using the 15" refractor of the George Agassiz Station Observatory of Harvard College, in Harvard, Massachusetts. The photographic emulsion used was Kodak IIa-O and the exposure time was typically forty-five minutes. Magnitudes wereobtained by eye-estimates using the sequence of comparison stars given by Angione(1971b) Magnitudes derived in this way have typical uncertainties of $\sim$.1 magnitude. The results for all four nights gave $m_b = 17.2 \pm .1$ and agree to within the uncertainties of measurement with the observations of Pomphrey et al.(1976) made during approximately the same time. Comparison of these results with the more recent data,shown in Figure 1, shows that the optical counterpart of 3C454.3 has been in a relatively quiescent state during the last three or four years, or at least has not undergone any strong sustained outburst. We will however continue to observe the source at Agassiz Observatory in order to detect any future outbursts.

The radiofrequency spectrum between 10 MHz and 100 Ghz is shown in Figure 2. References to the observations are given in the

figure caption. Because the flux at short centimeter wavelengths is highly variable, it was important to plot a set of measurements made as close to the same epoch as possible. Except for the observation at 90 GHz, all those above 1GHz (and some of those below) were made during early 1972.

The spectrum has been decomposed into four components such that the sum of the fluxes equals the level of the dashed curve. This decomposition is meant to be schematic only since the spectral characteristics of the individual components are not well determined from the total flux data alone. However, the strengths of the components have been drawn to match our VLBI results at 7.8 GHz and with total flux data at other frequencies, to be discussed in sections III and IV.

Below 100 MHz the emission is dominated by a steep-spectrum component ($\alpha \overset{*}{\sim} 1$) having an angular size greater than 1" (Bash,1968; Clarke et al.,1969; Readhead and Hewish,1976).

Between 100 MHz and ~ 1 GHz most of the flux is attributed to a component which becomes self absorbed near 400 MHz. Broten et al.(1969) observed the source at 610 MHz during 1969 with long-baseline interferometry and found that 60% of the flux originated in a component with an angular size ~".015 while the remainder came from an extended 1" component. Flux variations were observed in this frequency range during the late 1960's but since that time the flux has remained at a nearly constant level (Cotton 1975).

Above ~1 GHz VLBI and total flux observations show the presence

*The spectral index is defined such that $S \propto \nu^{-\alpha}$, where S=flux ν= frequency

of highly variable milliarsecond-size components.

Kellermann et al.(1971) and Broderick et al(1970) reported that their 5GHz single baseline data suggested a component $\sim 4 \times 10^{-3}$ in diameter containing 25-40% of the flux. Cohen et al.(1971) used a circular disk model to match their single baseline observations at 8 GHz,but stated that the fit was only fair and that the structure was probably more complex. Schilizzi et al.(1975a) fit their three baseline data at 10.7 GHz with a core halo model. Typical models have $\sim 3 \times 10^{-3}$ cores providing 60% of the total flux and $1\overset{''}{.}5 \times 10^{-3}$ that supply 10% while the remaining flux originates from a larger resolved source.

The most recent VLBI results are from Shaffer and Schilizzi (1975) who fit their single baseline observations at 1.7 GHz with a long narrow component , $\sim$.0095 by $\sim$.001 extended in position angle 115° and containing nearly all of the flux.

Although these early results demonstrated the compact nature of the source, the observations in most cases involved only a few measurements on a single baseline and consequently only very simple models could be justifiably used to fit the data. Clearly more detailed and systematic measurements were needed to ascertain both if the structure were more complex and if it changed with time.

II. OBSERVATIONS AND MODELLING PROCEDURE

During the MIT-Goddard Space Flight Center VLBI "Quasar Patrol" 3C454.3 and about 25 other sources have been observed since 1971. We report here the results of an attempt to model the source brightness distribution using correlated flux and closure-phase

data obtained during nine experiments extending from April 1972 to October 1974.

The observations were made at frequencies near 7.8 GHz with left circular polariztaion. A wide-band synthesis technique was employed (Rogers et al. 1970; Hinteregger et al. 1972) and observations were recorded with a Mark I VLBI recording system (Clark et al. 1968).

A description of the procedures for obtaining correlated flux and closure-phase and a discussion of the experimental errors has been given elsewhere (Rogers et al. 1974; Wittels et al., 1975)

Table I gives the dates and the antennas used for each experiment. There H,N,G and S refer, respectively, to the 120' antenna of the Haystack Observatory in Westford, Massachusetts; the 140' antenna of the National Radio Astronomy Observatory in Green Bank, West Virginia; the 210' antenna of the Jet Propulsion Laboratory in Goldstone, California; and the 85' antenna of the Chalmers University of Technology in Onsala, Sweden.

Before discussing our results, it will be instructive to describe a few details of how the source brightness distribution can be modelled using VLBI data.

The brightness B(x,y) of a source is related to the interferometric fringe amplitude and fringe phase by the Fourier transform relation

$$B(x,y)=\int\int V(u,v)e^{-2\pi i(ux+vy)}dxdy \qquad \text{II.1}$$

Here V(u,v) is the so-called complex visibility function whose amplitude and phase are the measured fringe amplitude and phase,respectively. X and y are the coordinates of the source on the plane of the sky measured along the east-west and north-

south directions, respectively, and u and v are the components of the baseline projected in the direction of the source, (expressed in some convenient units, for example milli-arcseconds per fringe) along the corresponding directions. As the earth rotates, V(u,v) is measured along an ellipse in the u-v plane, the available section of which is limited by the visiblity of the source at the telescopes.

Figure 3 shows the longest tracks for each of the six interferometer pairs used in the experiments. Locations which allow maxima and minima are enclosed by ellipses and rectangles, respectively. We point out that 3C454.3 never received as much coverage during a single experiment as shown here, however. The minimum fringe spacing, provided by the Goldstone-Sweden interferometer, was $\sim$.98 milli-arcseconds per fringe, sufficient to nearly completely resolve a Gaussian source $\sim$.50 milli-arcseconds in half-width.

If the source had an extent Δx and Δy in right ascension and declination then V(u,v) need only be sampled at points with a spacing of $2\pi / \Delta x$ in u and $2\pi/\Delta y$ in v. Equation II.1 could then be used to yield the brightness distribution. Presently this inversion is not performed using VLBI data because of two problems. First as Figure 3 clearly shows, only a few interferometer pairs are used and the sampling criterion is far from realized. Second, the source structure phase is not at the present time a measured quantity. The fringe phase is comprised of the phases introduced by clock errors, random fluctuations of the propagation paths due to atmosphere and ionosphere, instrumental

effects and by the structure of the source. At the present time there is not enough information to separate the individual phase contributions. However, if three or more antennas simultaneously observe the source, then source structure phase information can be obtained by calculating the so-called closure-phase which is freed from propagation medium effects, clock errors and instrumental effects. For three stations 1,2 and 3, the closure phase is defined as (Rogers et al. 1974)

$$\begin{aligned}\phi^{c}_{123} &= \phi^{m}_{12}(t_1) + \phi^{m}_{23}(t_2) - \phi^{m}_{13}(t_1) \\ &= \phi^{s}_{12}(t_1) + \phi^{s}_{23}(t_2) - \phi^{s}_{13}(t_1)\end{aligned} \qquad \text{II.2}$$

where the $\phi^{m}_{i,j}$ and $\phi^{s}_{i,j}$ are the fringe phases and structure phases on the i,j th baseline, measured at time t_i at site i. That the closure phase depends only on the structure phase follows since

$$\phi^{m}_{ij}(t_i) = \omega\Delta t_{i,j} \pm (\phi^{\theta}_{i} - \phi^{\theta}_{j}) + \phi^{s}_{i\,j} + 2n\pi \qquad \text{II.3}$$

where the $\Delta t_{i,j}$ are the total time delays (due to the contributions mentioned above) measured at site i relative to site j and ω is the (angular) radiofrequency. Using the information that

$$\Delta t_{i,j} + \Delta t_{j,k} - \Delta t_{i,k} = 0 \qquad \text{II.4}$$

which follows from the definition

$$\Delta t_{i,j} = t_i - t_j \qquad \text{II.5}$$

we arrive at equation II.2.

Because of these limitations one usually resorts to representing the brightness distribution as a parametrized model for the strengths, sizes, and positions of the individual components as determined by a best fit to the available data. This approach often yields a number of different models each of which satisfacorily

*The ϕ^{θ}_{i} are the feed position-angles, with positive sign for left and negative sign for right-circular polarization (IEEE convention).

fits the data and it is impossible to decide which of these, if any, is the "correct" model.

One can however, require that the models derived using data from different experiments be consistent with one another, i.e., that the brightness distribution change smoothly with time, if at all.

The models described in this paper were generated with a computer program developed by Bill Cotton at MIT. For this modelling scheme, the brightness distribution is represented by up to twenty circular Gaussian components located on a grid of positions in the sky. The model fitting procedure may be started by placing one component of arbitrary size and strength at some location on the grid. Both the size and strength of this component are then adjusted by a least-squares procedure. The program then attempts to add a second component to the brightness distribution by testing the component at all other grid points for the location that allows the best fit. When the optimum location is found, all parameters of the model are adjusted.

This procedure continues until either a specified number of components is added or until the quality of the fit is no longer improved by the addition of another component.

Often one can guess the approximate source structure from inspection of the maxima and minima on the u-v plane, or from a satisfactory model derived from a particular set of data. The solution can be started using this first-guess and the program may add to, delete or change components from the input model.

III. RESULTS

Correlated flux and closure phase data along with the predicted values from the derived models are shown in Figure 4. The total flux and model parameters for each epoch together with their 1-σ uncertainties are given in Table II and the brightness distributions themselves are presented in the form of contour diagrams in Figure 5.

Prior to the 1973 August experiment, 3C454.3 was observed with only the Haystack-Goldstone interferometer which provided a minimum fringe spacing of $2''\times10^{-3}$. These early curves of correlated flux-versus-time all have the same general shape, i.e. peaks at the endpoints near 1^h and 9^h GST with a broad minimum in between. The level of the maximum correlated flux is also seen to decrease from one experiment to the next, mimicking the decline in total flux.

Several two-component models were found to give good fits, however the one that is most consistent with those derived for later multiple-baseline experiments consisted of two unequal components, both in strength and in size, separated by about $4''\times10^{-3}$ along an axis with a position angle* of $\sim 135^\circ$. More complicated models could be used to give an even better fit but we feel that such models are not warranted given the limited amount of information. The principal maximum for this particular model, labelled $M_o(E)$, is drawn in Figure 3. The position angle is measured relative

* The position angle is measured counterclockwise, east of north on the plane of the sky.

to the larger and weaker component (component 1) having a strength of ~1.8 Jy* and a halfwidth at half power of $\leq 7 \times 10^{-3}$. Without phase information there is a 180^0 ambiguity in model orientation; however models for the multiple baseline experiments from which closure-phase could be calculated had component 1 situated northwest of component 2. The second component (component 2) had a half width at half power of $\leq 2 \times 10^{-3}$ and a strength that declined steadily from 10.5 Jy in 1972 April to 7.4 Jy in 1973 March. These models as do the later one account for all but 2.5-3 Jy of the total flux which ostensibly resides in a larger resolved halo.

The data from the next three multiple baseline experiments involving the Haystack, NRAO, Goldstone and Sweden antennas suggest that the structure is more complicated than that represented by this simple two-component model. Specifically, since the larger component is resolved by the Goldstone-Sweden interferometer, the Haystack-Goldstone-Sweden and NRAO-Goldstone Sweden closure-phase values would be zero for this model. The non-zero closure phase values imply that one of the components is not asymmetric in shape or that there are additional small components somewhere in the structure.

Unfortunately we lack extensive data for either the 1973 August or the 1973 October experiments and many of the maxima and minima are either absent or not well defined. Recording problems at NRAO and Sweden resulted in a large number of parity errors on the tapes and most of the data involving these two sites had to be discarded. Inparticular the NRAO-Sweden correlated fluxes had such large uncertainties that they were not used in the model fitting.

The remaining data were reasonably well fit by the previous double model with the addition of another small and weak (~1 Jy) component (component 3) located close to component 2. The location of this third component is not particularly well determined, although typical solutions indicated a separation of ~ $".6 \times 10^{-3}$ and a position angle of 70°-90° with respect to component 2. The strength of component 2 continued to decline following the trend of the earlier models. It should be noted that there are some discrepancies between this model and the data, particularly the Haystack-Goldstone-Sweden and NRAO-Goldstone-Sweden closure phases and the inability of the model to fit these data indicates that the source contains additional although probably weak structure.

The 1974 May experiment produced more correlated flux and closure phase data than did any other experiment. Unfortunately instrumental problems at Goldstone resulted in unreliable correlated flux data for the Haystack-Goldstone, NRAO-Goldstone and Goldstone-Sweden baselines and these were not used in the solution. There were, however, about eleven hours worth of Haystack-NRAO correlated flux data, more than for either the 1973 August or 1973 October experiment.

If we assume that the peak on the Haystack-NRAO curve near 8^{h}GST lies on the principal maximum, then by referring to Figure III, it can be seen that the angle between th +v axis and the principal maximum labelled $M_{o}(L)$ is $\sim 20^{\circ}$ less than the +v axis and the principal maximum $M_{o}(E)$ drawn for the earlier data. This change indicates, independent of any modelling, that the position angle of the overall structure has decreased since the

earlier epochs. Fits gave, in addition to the previous three-component model, yet another weak and relatively small 1 Jy component (component 4) separated by $5\overset{''}{.}5 \times 10^{-3}$ and with a position angle of 117° with respect to component 1. Between October 1973 and May 1974 the total flux increased by ~ 1 Jy (the source was undergoing an outburst which peaked during late 1974) and so it is not unexpected that another component would appear in the structure.

Solutions also indicated that between the 1973 October and 1974 May experiments the strength of component 2 decreased by 1.5 Jy while the strength of component 3 increased by about the same amount. Components 2 and 3 might then be either two spatially separated although relatively close sources, each of which have undergone independent outbursts or they may be part of a single elliptically shaped source that began to brighten at one end between October 1973 and May 1974. Unfortunately there is not enough information from the single baseline data to tell, reliably, if component 3 existed or not during the earlier epochs.

That components 1,2 and 4 (treating components 2 and 3 as a single object) deviate from collinearity by $\sim 20^{\circ}$ is itself an interesting result since the total structure for two other multi-component sources namely 3C273 and 3C279 appears to be collinear to within $\sim 5^{\circ}$. (Schilizzi et al. 1975; Cotton et al. 1976; Geller, 1976).

During the 1974 experiment the source was observed with only the Haystack-NRAO interferometer but received about 10 hours worth of coverage. The shape of this correlated flux curve is similiar

to that of the 1974 May experiment although the level increased by ~ 2 Jy, approximately the amount by which the total flux increased.

It was sufficient to fit these data with only two large components, separated by roughly the distance between and at about the same position angle as components 1 and 4 of the 1974 May model. The relatively large angular size of both components is a result of the lower angular resolution provided by the Haystack-NRAO interferometer; the stronger component is most likely comprised of components 2,3 and 4 of the previous models. Because of the lower resolution, however, we consider this model to be at least qualitatively consistent with the others.

IV DISCUSSION

Examination of our results toute ensemble reveals that the compact structure of 3C454.3 consists of several components some of which have undergone changes in their strength during the span of the observations. The projected linear distance between the two outermost components is ~ 50 parsecs and the component diameters range in size from 3 to 10 parsecs. While it is possible to provide qualitative estimates for the sizes, strengths and positions of the individual components it is difficult to determine these parameters accurately because of a lack of extensive data. These models are however consistent with total flux variations which indicate or at least suggest that changes in structure have occurred. Before we discuss these variations we would like to mention the following points.

The position angle of the most widely separated components agrees to within 2° with the orientation of the single elliptically shaped source suggested by VLBI observations of Shaffer and Schilizzi (1975) at 1.7 GHz. The

total angular extent of their model is greaterthan ours however, $9''.x10^{-3}$ compared to $5''.5x10^{-3}$. The obvious interpretation of these results is that the compact structure is embedded within a larger and therefore older source, both of which have become extended, via some unknown physical mechanism, along the same direction. Surrounding these sources is yet another 1" halo that dominates the emission below 100 MHz but that contributes a negligible amount of flux above ~1 GHz. This picture is not unique, for radio and optical observations of the active galaxy 3C84 have shown that this source possesses a hierarchy of structure that is approximately aligned over an angular scale of several minutes of arc (Riley and Perola 1975). As more results become available in fact, it appears that the alignment of small and large scale structure may be a characteristic feature of active QSO's, galaxies and radio galaxies. Obviously additional VLBI observations of 3C454.3 at lower frequencies would be useful to determine if the structure of the extended component consists of more than a single elongated blob.

Another interesting point concerns the relationship between the source structure and the magnetic field direction. Haves(1975) has used polarization observations between 73 cm and 2cm to estimate values of rotation measure and intrinsic polarization angle for a number of extragalactic sources. For 3C454.3 he finds an intrinsic polarization angle of $23^{o}\pm2^{o}$, a value that is nearly perpendicular to the major axis of the source. For an optically thin (thick) source the polarization vector is perpendicular (parallel) to the magnetic field direction (eg. Aller 1970). In Figure 6 we have plotted the polarized flux spectrum using the data obtained from the sources listed in the figure caption. The measurements marked by . were all made at various times between 1964 and 1976 and fall along a smooth curve with a turnover near 1GHz and a spectral index ~.6. The observations marked by X were all made at a time of an outburst in 1967-1968 and are all noticeably

higher than those which fall along the curve. Observation at 2.7 GHz and at 8 GHz by Wardle and Altschuler (1976) show that the polarized flux remained constant during two outbursts that occurred in 1972 and 1974. These observations indicate that the polarized flux may arise from a quiescent source and that some but not all of the outbursts may be polarized. As we will show in Section VI, the spectral component having a turnover near ~ 2 GHz is possibly associated with the source which varied during the late 1960's so that the quiescent source is likely identified with the component having the peak near 400 MHz. The polarized flux turnover near 1 GHz is an indication that Faraday depolarization may be occurring in the source or in the 1"halo (Burn, 1966; Goldstein, 1968). Since this source is optically thin at the higher frequencies, the source structure is extended in the direction of the the average magnetic field. Haves and Conway (1975) have found that for those sources with a well defined major axis of symmetry, the majority exhibit polarization angles which lie nearly perpendicular to the axis.

These models provide evidence that component 4 may have "turned on" sometime between October 1973 and May 1974. We tried a solution using the 1973 October data set that included component 4 as part of the input model with the result that the program effectively deleted this component from the model but did give the three-component model described earlier. On the other hand the 1974 May and 1974 October Haystack-NRAO maxima and minima indicate structure on a larger angular scale and at a different position angle than those on the earlier single baseline curves.

The origin of component 4 is a mystery however. An attempt to explain it as the result of an ejection from its nearest neighbor, componont 3, would (assuming the time of ejection to be as early as October 1973) require these two components to have an apparent separation velocity of at least 150c, more

than an order of magnitude larger than the velocities suggested for any other source. It is possible of course to reduce this large velocity requirement by postulating a much earlier ejection time when the component was weak so as to escape detection until May 1974.

An alternative explanation is the "Christmas tree lights " model developed by Dent (1972) in which outbursts are spatially independent events that occur at random throughout the source. This hypothesis has had difficulty explaining the apparent superrelativistic motions of components in other sources since they have always been observed to separate and never contract. With the available data however there is no way of deciding between these two explanations. Apart from the former interpretation our models show no evidence for superrelativistic expansion of any of the components. As a final note we stress that the orientation of components 1,2 and 4 does deviate from collinearity by $\sim 20^{o}$ and so any proposed ejection-type mechanism which predicts a configuration of strictly aligned components is not satisfactory for explaining the morphology of the entire source.

V ESTIMATE OF PHYSICAL PARAMETERS

It is possible in principle to obtain estimates of some of the physical characteristics of a synchrotron-emitting cloud from the spectral and VLBI model parameters. The average magnetic field, B, within the source may be estimated given the angular radius θ_s , the frequency ν_a at which the source becomes self-absorbed and the flux S_a at this frequency (eg. Jones and O'Dell, 1974)

$$B^{1/2} = 2mi_{\alpha 0}\nu_a^{5/2}(2\pi m/e)^{1/2}\ \pi\theta_s^2(\sin\theta_o)^{-1/2}(1+z)^{-1/2}\ S_a^{-1}\ \gamma_o^{1/2} \qquad V.1$$

Here, m and e are the mass and charge of the electron, respectively, θ_o is the angle of the observed radiation with respect to the magnetic field ($\sin\theta_o \sim 1$ for electron isotropy), $i_{\alpha 0}$ is a dimensionless constant of order unity, tabulated by Jones and O'Dell, which depends on spectral index, z the redshift of the

source and γ_o is the Lorentz factor, $(1-v^2/c^2)^{-1/2}$, which accounts for a possible relativistic expansion of the cloud. The effects of a relativistic expansion on the magnetic field and radiation density have been discussed by Rees and Simon (1968). B, ν_a, S_a and θ_s are expressed in units of Gauss, Hz, erg/cm^2 sec Hz, and radians, respectively.

Because of the strong functional dependances on the observed quantities especially angular size and turnover frequency, it is difficult to calculate B accurately. Also, this expression will provide only an upper limit to the magnetic field since it was derived under the assumption that the spectral turnover is due only to synchrotron self-absorption. If the turnover is caused by other mechanisms, then ν_a will be overestimated and S_a underestimated implying a true magnetic field much smaller than that given by Equation V.1. As will be discussed in the next section, some other process other than self-absorption is required to suppress the expected variations at 2.7 GHz although the effect might be unimportant at the observed turnover frequency. Using $\theta_s = 2\times10^{-3}$, $\nu_a = 9$ GHz and $S_a = 10.5$ Jy we calculate the average magnetic field to be $B \cong 1.\times10^{-2} (\sin\theta_o)^{-1} \gamma_o$ Gauss.

The energy density of the radiation field is given by the relation (Burbidge, Jones and O'Dell, 1974)

$$U_r = \frac{4\nu_n S_n}{\theta_s^2 c} \frac{1}{1-\alpha} \left[\left(\frac{\nu_u}{\nu} \right)^{1-\alpha} - 1 \right] \frac{\Omega_e}{4\pi} \frac{(1+z)^4}{\gamma_o^4} \qquad V.2$$

Here, Ω_e is the solid angle over which the emission is distributed locally ($\sim 4\pi$ for a disordered field or electron anisotropy). The radiation density depends on the the upper cutoff frequency ν_u, corresponding to the cutoff energy in the electron energy distribution. From the spectrum in Figure 2 we estimate ν_u to be at least 100 GHz, although it probably lies farther in the millimeter region where to our knowledge measurements were never made or

never published. Our calculations yield $U_r = 4.7\times10^{-3}\,\Omega_e/4\pi/\,\gamma_o^4$ erg/cm^3 for ν_u =100 GHz. The magnetic energy density, $B^2/8\pi = 4\times10^{-6}(\sin\theta_o)^{-2}\gamma_o^2$.

One can show however that if $\sin\theta_o = 1$, $\Omega_e \cong 4\pi$ and $\gamma_o \cong 1$ then these energy densities would result in an unacceptably large Compton-scattered flux at optical wavelengths. The ratio of Compton-scattered to synchrotron flux is given by (eg. Peterson and King, 1975)

$$\frac{F_c}{F_s} = \frac{1.26\times10^7}{\nu_u}\ln\left(\frac{\nu_u}{\nu_l}\right)\left(\frac{\nu_c}{\nu_s}\,\frac{1.05\times10^6}{\nu_s}\right)^{\frac{1-\gamma}{2}} \qquad \text{V.3}$$

$$\times\,\frac{(\gamma^2+4\gamma+11)(3-\gamma)}{(\gamma+3)^2(\gamma+1)(\gamma+5)}\,\frac{U_r}{U_m}\,\beta^{\frac{3-\gamma}{2}}$$

Here ν_u and ν_l are the upper and lower cutoff frequencies in the electron energy distribution, F_c and F_s are the Compton and synchrotron fluxes at frequencies ν_c and ν_s, respectively and γ is the power law index of the electron energy distribution, related to the spectral index by $\gamma = 1+2\alpha$. The lower cutoff frequency cannot be estimated directly from the spectrum as synchrotron self-absorption and or other processes cause the spectrum to turn over above where the effect of a low energy cutoff would be manifest. (A low energy cutoff would cause the flux to decrease as $\nu^{1/3}$ below the peak, a rate that is definitely less steep than observed.) Many extended sources do show departures from a normal power law specrtum in the range of ten to a few hundred MHz (eg. Kellermann, 1966; Moffet, 1976) and a lower cutoff frequency of 10 MHz is often assumed. With $\gamma = 1.5$, $F_s = 10.5$ Jy and with $\sin\theta_o = 1$, $\Omega_e = 4\pi$ and $\gamma_o = 1$, then the Compton flux would be $F_c \sim 4\times10^{-2}$ Jy at 7×10^{14} Hz (4300 Å), corresponding to an optical magnitude* of 12.4.

The magnitude during 1972 was ~17, so it is difficult to reconcile the predicted brightness with observations unless one invokes some combination of small pitch angles, anisotropic emission or relativistic expansion. A calculation shows that in order for relativistic expansion to erase the discrepancy, then

*The conversion from flux to B magnitudes is $m_B = -2.5\,\mathrm{Log}(F_c) - 48.55$ where F_c is expressed in units of erg/cm^2-sec-Hz.

γ_e must be greater than ~ 2 ,corresponding to an expansion velocity of .7c. On the other hand a small pitch angle explanation would require the angles to be less than 8^o.

VI TOTAL FLUX VARIATIONS

The spectral decomposition shown in Figure 2 agrees with our VLBI model results during early 1972. We first associate the variable high frequency source with component 2 which had a strength of 10.5 Jy in April 1972. Next we assume that the 3 Jy halo is the source having the spectral turnover near ~ 400 MHz. Finally we associate the larger low brightness VLBI component with the component having a turnover near 2 GHz. The spectral turnover of component 2 is rather uncertain although it appears to occur near 1GHz. The spectral index of each component is drawn next to the corresponding curve in Figure 2.

Figure 7 shows the total flux variations between 1970 and 1976 at 2.7,7.8, 15.5 and 31.4 GHz. Our VLBI observations are indicated by arrows on the abscissa. (Between 1965 and 1969 the source also underwent a strong outburst; We will discuss this particular event later on in this section.)

The observations at 7.8 GHz show evidence for three outbursts, labelled A,B and C. Following Dent and Hobbs (1972) a line has been drawn through the six measurements at 31.4 GHz to suggest that there may have been two outbursts between 1970 and 1972.

Outburst A is relatively weak and not well defined particularly at 15.5 GHz and 31.4 GHz; it seems to have peaked circa May 1971 at 7.8 GHz and sometime sooner at the two higher frequencies. As outburst A declined, outburst B, the strongest of the three, began during July 1971. The peak of this outburst occurs near April 1972 and is nearly simultaneous at 7.8, 15.5 and 31.4 GHz. The data at 2.7 GHz conspicously show no evidence for variations at any

time.

We clearly associate outburst B with component 2 in our models since the decline in total flux of the latter mimics the decline in total flux.Because of its relatively large size and nearly constant strength, component 1 is presumably the remnant of a recent outburst and as we will demonstrate below, could be the one which occurred during the late 1960's. Outburst C is probably associated with the increase in strength of either component 4 or component 3 or perhaps both.

The properties of outburst B are not consistent with those predicted by the model proposed by van der Laan (1966) to explain flux variations of compact sources. For this model an explosive event causes a cloud of relativistic electrons to be ejected instantaneously at a point within the source;the electrons are accelerated in an ambient magnetic field and radiate via the synchrotron mechanism. It is assumed that the the electrons have an energy distribution of the form

$$N(E)dE \propto E^{-\delta} dE \qquad \text{VI.1}$$

and confined to the range $E_1 < E < E_2$. $N(E)dE$ is the number of electrons with energy between E and E+dE and δ is a power law index. Initially the expanding cloud is sufficiently compact to be optically thick at all radio-frequencies. As the cloud expands magnetic flux is conserved and the relativistic gas cools adiabatically.

The relationship between flux S and the observation frequency ν can be expressed in the following manner (van der Laan,1966)

$$S(\nu,\rho) = \frac{S_{mo} (\nu/\nu_m)^{5/2} \rho^3 (1-\exp(-\tau_m(\nu/\nu_m)^{-\gamma+4/2 -2\gamma+3}))}{1-\exp(-\tau_m)} \qquad \text{VI.2}$$

Here ρ is the relative radius of the source, r/r_o where r_o is the radius at an arbitrary epoch. S_{mo} is the maximum flux at that epoch and ν_m is the frequency at which the flux is a maximum. τ_m, the optical depth corresponding to ν_m is the solution of

$$e^{-\tau_m} - \frac{\gamma+4}{5}\tau_m - 1 = 0 \qquad \text{VI.4}$$

With $\gamma = 1.5$, $\tau_m = .26$.

Figure 8 shows the predicted flux as a function of ρ at 2.7, 7.8 15.5 and 31.4 GHz calculated assuming that $\nu_m = 9$GHz and $S_{mo} = 10.5$ Jy. Here $\rho = 1$ corresponds to the radius during April 1972. Van der Laan's model predicts that as the initially optically thick source expands, an outburst will be observed first at some high frequency then progressively later with decreased amplitudes. Below ν_m, the source is optically thick due to self-absorption and the flux variations decrease as $\nu^{5/2}$, independent of γ . With the assumed values, the flux should have peaked near ~70 Jy at 31.4 GHz when the relative radius was .4; at 15.5 GHz the maximum flux should have reached ~29 Jy when ρ was ~.6. These predictions are in obvious contradiction with the observations which show both that the outburst peaks nearly simultaneously at the three highest frequencies and has a greater amplitude at 7.8 GHz than at either 15.5 and 31.4 GHz.

The high frequency discrepancy can be explained only if the source was initially optically thin down to ~ 8 GHz so that the flux variations would decrease as $\nu^{-\alpha}$ at the higher frequencies. The increase in intensity would be due to an increase in the number of radiating particles. The duration of the increase

is then determined by the length of time over which new particles are continuously injected while the rate of increase is determined by the balance between the injection rate and the various loss mechanisms, such as expansion of the cloud.

We have attempted to fit the observations with a prolonged injection model, first discussed by Peterson and Dent (1973). The form of the variations with time can be expressed as

$$S(\nu,t) = a(t+\rho)^{3}\,\nu^{\frac{5}{2}}\,(1-e^{-\tilde{\tau}})$$
$$\tilde{\tau} = b(t+\rho)^{-2\gamma-3}\,\nu^{-\frac{\gamma+4}{2}}\,F(t) \qquad \text{VI.5}$$

Here, a and b are constants to be determined by a fit to the data; $\rho = r_o/v$ where r_o and v are the initial size and expansion velocity of the cloud. The initial size is interpreted as the radius of the source when the model first becomes applicable. The parameter ρ must be introduced since the source does not necessarily expand from a point. F(t) is a function that exhibits the effect of the injection. The form that we have considered describes a peaked injection model and is given explicitely by

$$t > 0 \quad f(t) = \arctan(\gamma/\epsilon) + \arctan(t-\gamma/\epsilon)$$
$$t < 0 \quad f(t) = 0 \qquad \text{VI.6}$$

For this form, γ is the time when the injection rate is a maximum and ϵ is related to its duration.

Equations VI.5 and VI.6 were used to solve for a, b, ρ, γ, and ϵ by a least-squares fit to the data after the frequency dependent contributions from the two background components described earlier were subtracted off. A number of combinations of t_o (the time when the injection begins) and δ were tried.

The results for t_o=1971.0 and γ =1.5 which seemed to give the best fit are shown in Figure 9. It can be seen that there is now good agreement between the model and the higher frequency data; the prolonged injection has allowed the source to be optically thin above 8 GHz during the early development of the outburst. In this model, the values of χ and ϵ imply that the maximum injection rate occurred ~1972.1 and that the buildup of particles lasted ~.5 years. The value of ρ =1.05 indicates that for v=.7c, the initial size r_o must have been ~.2 parsecs. The model is however unable to account for the absence of variations at 2.7 GHz but we will offer an explanation for this below.

We also fit the 1960's outburst with the same peaked injection model since our calculations show that the canonical model fails for it as well. One of the best fits, with t_o=1965.2 and γ =1.7 is shown in Figure 10. The values of χ and ϵ imply that the maximum rate of injection occurred near 1967.6 and that the effective width of the injection peak was ~.7 years. Extrapolating the 8 GHz flux we find that this component would have had a strength of ~ 2.5 Jy in 1972.0 and 1.5 Jy in 1973.0. These values are in reasonable agreement with the strength of the larger VLBI component leading us to suspect that this component is the remnant of the 1960's outburst.

Although there is generally good agreement between the model and the observations, there are some systematic differences, especially for the early 2.7 GHz data where the flux is ~ 3 Jy higher than predicted. This discrepancy could be the result of our failure to subtract enough background flux at this

frequency or it could be due to some deficiency in the model. Wepoint out that the peaked injection form is not unique,and we are currently trying to fit the outbursts with other simple functions.

The major discrepancy betweeen the model and the observations is that one should have observed a 4-5 Jy outburst at 2.7 GHz during the 1971 outburst although the data are consistent with an upper limit of ~.5 Jy for any variations at this frequency, Thus if we believe that the prolonged injection model can adequately describe the higher frequency behavior, then one must invoke some process other than self absorption to suppress these variations.

Perhaps the simplest mechanism to understand, but by no means the only one, is that of thermal absorption. If a layer of ionized hydrogen is located between the source and the observer, then the power law spectrum will be attenuated by thermal absorption within the cloud in the following way.

$$S \propto \nu^{-\alpha} e^{-\tau_a} \qquad \text{VI.7}$$

Here, S is the observed flux and τ_a is the optical depth due to thermal absorption and is given by

$$\tau_a = 3 \times 10^{18} \nu^{-2.1} N_e^{2} d \qquad \text{VI.8}$$

Here, T_e is the electron kinetic temperature within the ionized region, N_e is the electron density, ν is the frequency of observation, expressed in Hz, and d is the path length through the cloud, expressed in parsecs. From the predicted and observed upper limits for variations at 2.7 GHz, $e^{-\tau_a} \sim 1/8$, so $\tau_a = 2.2$. At 9 GHz the optical depth is .15 so that our previously determined value for the magnetic field should be decreased. After we

corrected for the frequency dependence of the thermal absorption we found that τ_a would have occurred near ~7 GHz and that the peak flux was ~ 13 Jy, yielding a magnetic field $B \approx 2 \times 10^{-3} \sin\theta_o^{-1} \delta_o$ gauss.

If we adopt a n electron temperature of 10,000°K, then $N_e \approx 6.5 \times 10^3 \, d^{-1/2} \, cm^{-3}$. The path length d is unknown, however if we believe our VLBI results, then a rough estimate can be made using the following simple argument.

If thermal absorption is also responsible for the lack of variations during outburst C, then we could infer that the cloud which lies in front of or perhaps surrounds component 2 possibly covers component 4 as well. (It is also assumed that outburst C is attributed to the appearance of component 4.) If so then the spatial extent of the cloud would be at least 20 parsecs, i.e. the projected distance between the components. If, for example, the region is a sphere of radius 20 parsecs, then $N_e \approx 1.5 \times 10^3 \, cm^{-3}$. Two important points should be made here, however. If the thermal absorption interpretation is correct, then the plasma density must be non-uniform over the region containing the compact components, since as Figure 10 clearly shows, the source varied considerably at 2.7 GHz during the 1960's outburst. Specifically, if we have correctly guessed that component 1 is the remnant of this outburst, then our VLBI results would indicate the presence of more thermal plasma at the south-eastern end of the source than at the northwestern end, corresponding to a distance of only 50 parsecs.

It is also possible to compare the electron density crudely estimated here with any value suggested by optical spectro-photometry. Unfortunately the spectrum has not been studied

nearly as carefully as the optical continuum. Visvanathan (1973) has measured the CIII] λ1909/MgII λ2800 intensity ratio to be ~ 2. Chan and Burbidge (1975) report the presence of the [NeV] λ3426 line but claim that no other forbidden lines are seen in the spectrum. Based on models for line-emitting regions in QSO's and Seyfert galaxies (eg. Davidson(1972), MacAlpine (1972), Chan and Burbidge (1975)), these observational results would tend to suggest that the lines are formed in relatively high density regions, having $N_e \sim 10^6$-10^7 cm^{-3}, where collisional de-excitation of the forbidden line levels is important. Thus for the line emitting regions to lie in front of the radio components, the path length would have to be, assuming $N_e = 10^6$ cm^{-3}, only 4×10^{-5} parsecs. This exceedingly small thickness can probably be ruled out since the large internal velocities (20,000-30,000 km/sec) implied by the line widths (Visvanathan,1973) would quickly disrupt the region.

High sensitivity studies of optical spectra of the nuclei of Seyfert galaxies and low redshift QSO's have in fact suggested that the line-emitting regions are not uniform in either density or spatial extent, but rather are in the form of filaments or individual clouds having densities that range from 10^2-10^8 cm^{-3}. (Ulrich,1973;Oke and Shields,1976;Shields and Oke,1975; Glaspy et al. 1976; and Baldwin,1975). Perhaps higher sensitivity spectrophotometric studies might be able to put limits on the strengths of the forbidden and other lines and thus on the existence of a lower density component. Needless to say, however, the thermal absorption interpretation is very speculative and additional VLBI studies, coupled with total flux and optical observations are required to understand the problem.

REFERENCES

Aller,H.D.,1970,Ap.J.,161,19.

Altschuler,W.R ,and Wardle,J.F.C.,1976,Memoirs,MNRAS,82,1.

Angione,R.J.,1971a,A.J.,76,25.

Angione,R.J.,1971b,A.J.,76,412.

Bash,F.N.,1968,AP.J.suppl.,16,373.

Baldwin,J.,1975,AP.J.,201,26.

Berge,G.L.and Seilstad,G.A.,1969,Ap.J.,148,367.

Bignell,R.C.and Seaquist,E.R.,1973,A.J.,78,536.

Broderick,J.J.,Vitkevitch,V.V.,Jauncey,D.L.Efanov,V.A.,Kellerman, K.I.,

Burbidge,G.R.and Burbidge,E.M.,1967,Quasi Stellar Objects, San FRancisco,Freeman Press.

Burn,B.J.,1966,MNRAS,133,67.

Clark,B.G.,Kellerman,K.I.,Bare,C.C.,Cohen,M.H. and Jauncey,D.L., 1968,Ap.J.,153,705.

Broten,N.W.,Legg,T.H.,Clarke,R.W.,Locke,J.L.,Galt,J.A.,Yen, Y.A.,and Chisholm,R.M.,1969,MNRAS,146,313.

Cohen,M.H.,Moffet,A.T.,Romney,J.D.,Schilizzi,R.T.,Seilstad,G.A., Kellerman,K.I.,Purcell,G.H.,Shaffer,D.B.,Pauliny-toth,I.I.K, Preuss,E.,Witzel,A.,and Rinehart,R.,1976,D.B.,AP.J. Lett., 206,L1.

Clark,B.G.,Kellerman,K.I.,Cohen,M.H.,Shaffer,D.B.,Broderick,J.J., Jauncey,D.L.,Matveyenko,L.I., and Moiseyev,I.G.,1973,

Cohen,M.H.,Cannon,W.,Purcell,G.H.,Shaffer,D.B.,Broderick,J.J., Kellerman,K.I.,and Jauncey,D.L.,1971,Ap.J,170,207.

Cotton,W.D ,1975,PhD Thesis, University of Texas.

Cotton,W.D.,Counselman,C.C.,III,Shapiro,I.I.,Wittels,J.J.,
Hinteregger,H.F.,Knight,C.A.,Rogers,A.E.E.,Whitney,A.R.,
Clark,T.A.,Hutton,L.K.,Ronnang,B.O.,Rydbeck,O.E.H.,Neill,A.E.,
Klemperer,W.K.,and Warnock,W.W.,1976 in preparation.

Conway,R.G.,Gilbert,J.A.,Kronberg,P.P.,and Strom,R.G.,1972,
MNRAS,157,443.

Davidson,K.,1972,Ap.J.,171,213.

Dent,W.A.,1972, Ap.J. Lett.,175,L55.

Dent,W.A.,and Kajoian,G.,1972, A.J., 77,819.

Dent,W.A., and Hobbs,R.W.,1973,A.J.78,163.

Dent,W.A.,Kapitzky,J.E., and Kajoian,G.,1974,A.J.,1232.

Fogarty,W.H.,Epstein,E.E.,Montgomery,J.W.,and Dworetsky,M.,
1971,A.J.,76,537.

Gardner,F.F.,Morris,D.,and Whiteoak,1969a,Aust. J. Phys.,22,79.

Gardner,F.F.,Whiteoak,J.B.,and Morris,D.,1969b,Aust. J. Phys.,
22,821.

Geller,R.B.,1976, Masters Thesis, Massachusetts Institute of
Technology.

Glaspy,J.W.,Eilek,J.A.,Fahlman,G.G.,and Auman,1976,Ap.J.,203,335.

Goldstein,S.J.,1968,Ap.J.,151,65.

Haves,P.,1975,MNRAS,173,553.

Haves,P.and Conway,R.G.,1975,MNRAS,173,53p.

Harris,D.E.,1974,A.J.,79,1211.

Hinteregger,H.F.,Shapiro,I.I.,Robertson,D.S.,Knight,C.A.,
Whitney,A.R.,Rogers,A.E.E.,Moran,J.M.,Clark,T.A.,and Burke,
B.F.,1972, Science,178,396.

Hunstead,R.W.,1972, Ap.J.Lett.,12,193.

Jones,T.W.,O'Dell,S.L.,and Stein,S.L.,1974,Ap.J.,188 353

Kellerman,K.I.,Jauncey,D.L.,Cohen,M.H.,Shaffer,D.B.,Clark,B.G.,

Romney,B.,Rydbeck,O.E.H.,Matveyenko,L.,Moiseyev,I.G.,Vitkevitch,V.V., Cooper,B.F.G.,and Batchelor,R.,1971,Ap.J.,169,1.

Hobbs,R.W.and Waak,J.A.,197 ,A.J.,77,342.

Lu,P.K.,1972,A.J.,79,1211.

Lynds,C.R.,1967,Ap.J.,147,837.

MacAlpine,G.M.,1972,Ap.J,175,11.

McCullough,T.P.,and Waak,J.A.,1969,Ap.J.,158,849.

McGimsey,B.O.,Smith,A.G.,Scott,R.L.,Leacock,R.J.,Edwards,P.L., Hackney,R.L.,and Hackney,K.R.,1975,A.J.,80,895.

Medd,W.J.,Andrew,B.H.,Harvey,G.A.,and Locke,J.L.,1972,MNRAS, (Memoirs),77,109.

Moffet,A.T.,1976,Galaxies and the Universe,University of Chicago Press.

Oke,J.B.,and Shields,G.A.,1976,Ap.J.,207,713.

Pomphrey,R.B.,Smith,A.G.,Leacock,R.J.,Scott,R.L.,Olooock,J.T., Edwards,P.,and Dent, W.A.,1976,A.J.,81,489.

Readhead,A.C.S.,and Hewish,A.,1976,MNRAS,176,571.

Rees,M.,and Simon,M.,1968,Ap.J. Lett.,152,L145.

Rogers,A.E.E.,197 ,Radio Science,5,1239.

Rogers,A.E.E.,Hinteregger,H.F.,Whitney,A.R.,Counselman,C.C.,III,Wittels, J.J.,Shapiro,I.I.,Klemperer,W.K.,Warnock,W.W.,Clark,T.A., Hutton,L.K.,Marandino,G.E.,Romney,B.O.,Rydbeck,O.E.H.,and Neill.A.E.,1974,Ap.J.,193,293.

Roberts,J.A.,Roger,R.S.,Ribes,J.C.,Cooke,D.J.,Murray,J.D.,Cooper, B.F.,and Biraud,F.,1975,Aust. J. Phys.,28,325.

Ryle,M.,O'Dell,D.M.,and Waggett,1975,MNRAS,173,9.

Selmes,R.A.,Tritton,K.P.,1975,MNRAS,170,15.

Schilizzi,R.T.Cohen,M.H.,Romney,J.D.,Shaffer,D.B.,Kellerman,K.I.,
Swenson,G.W.,Yen,J.L.,and Rinehart,R.,1975a,Ap.J.,201,256.

Schilizzi,R.T.,Cohen,M.H.,Romney,J.D.,Shaffer,D.B.,Kellerman,K.I.,
Swenson,G.W.,Yen,J.L.,and Rinehart,R.,1975b,Ap.J., 201,263.

Shaffer,D.B.,and Schilizzi,R.T.,1975,A.J., 80 753.

Shields,G.A.,and Oke,J.B.,1975,Ap.J., 197,5.

Slee,O.B.,and Higgins,G.S.,1973,Aust. J. Phys.,27,1.

Tabara,H.,Morris,D.,Kawajiri,N.,and Kanno,M.,1972, Publ.,
Astron. Soc. Japan,24,301.

Ulrich,M.H.,1973,Ap.J.,181,51.

van der Laan,H.,1966,Nature,211,1131.

Visvanathan,N.,1973,Ap.J.,179,1.

Walker,M.F.,1968,Ap.J.,151,71.

Whitney,A.R.,Shapiro,I.I.,Rogers,A.E.E.,Robertson,D.S.,Knight,C.A.,
Clark,T.A.,Goldstein,R.M.,Marandino,G.E.,Vandenberg,N.R.,
1971,Science ,173,225.

Wittels,J.J.,Knight,C.A.,Shapiro,I.I.,Hinteregger,H.F.,Rogers,A.E.E.,
Whitney,A.R.,Clark,T.A.,Hutton,L.K.,Marandino,G.E.,Neill,A.E.,
Romney,B.O.,Rydbeck,O.E.H.,Kle,perer,W.K.,and Warnock,W.W.,
1975,Ap.J.,196,13.

Wittels,J.J.,Cotton,W.D.,Counselman,C.C.,III,Shapiro,I.I.,
Hinteregger,H.F.,Knight,C.A.,Rogers,A.E.E.,Whitney,A.R.,
Clark,T.A.,Hutton,L.K.,Romney,B.O.,Rydbeck,O.E.H.,and
Neill,A.E.,1976,Ap.J.Lett.,206,L75.

Witzel,A.,and Veron,P.,1971,Astrophys. Lett .,7,225.

Burbidge,G.R.,Jones,T.W.,and O'Dell,S.L.,1974,Ap.J,193,43.

Peterson,F.W.,and King,C.F.,III,1975,Ap.J.,195,753.

Table I.

List of Experiments

Date	Antennas
1) 1972 April 14,15	H-G
2) 1972 August 29,30	H-G
3) 1972 November 7	H-G
4) 1973 February 4,5	H-G
5) 1973 March 30,31	H-G
6) 1973 August 10-14	H-N-G-S
7) 1973 October 12-16	H-N-G-S
8) 1974 April 29-May 3	H-N-G-S
9) 1974 October 27,28	H-N

TABLE II

Source Models

Date	Total Flux Density (Jy)	Component #	Flux Density (Jy)	HWHP ($\times 10^{-3}$")	Separation ($\times 10^{-3}$")	Position Angle (Degrees)
4-72	15.5± 1.1	1	(2.0)	(.59)		
		2	(10.5)	(.27)	(3.7)	(130.6)
8-72	13.4±.34	1	2.0±1.0	.98±.17		
		2	9.0±.16	.18± .08	4.0±.05	143±1.2
11-72	13.2±.7	1	1.8±2.5	.68±.4		
		2	8.2± 1.1	.20± .12	3.69±.07	130±2.0
2-73	11.9±.6	1	1.8±2.5	.74±.45		
		2	7.3±.63	.24±.07	3.83±.04	139±.7
3-73	11.7±.6	1	1.7±1.1	.75±.23		
		2	7.5±.35	.3±.03	4.24±.08	139±.9

*Model parameters for April 1972 are very uncertain and thus no formal error is given.

Date	Total Flux Density (Jy)	Component #	Flux Density (Jy)	HWHP ($\times 10^{-3}$")	Separation ($\times 10^{-3}$")	Position Angle (Degrees)
8-73	9.9±.5	1	1.7±.2	.8±.16		
		2	4.9±.02	.25±.06	3.68±.06	135±1.3
		3	.92±.08	.12±.37	4.0±.05	122.8±.7
10-73	10.0±.5	1	1.6±.2	.83±.17		
		2	4.7±.03	.37±.02	3.54±.03	132±.2
		3	1.0±.02	.12±.12	4.12±.02	129±1.0
5-74	11.0±.4	1	2.0±.14	.67±.14		
		2	3.4±.02	.38±.24	3.6±.1	132±1.5
		3	1.9±.13	.19±.10	4.12±.09	129±.8
		4	1.1±.07	.32±.13	5.6±.06	117±.8
10-74	13.7±.5	1	1.8±.8	.74±.79		
		2	8.9±.5	.56±.73	4.4±.41	114±7.1

FIGURE CAPTIONS

Figure 1. The optical variations of 3C454.3 between 1968 and 1975 plotted as blue magnitude versus time. Data were obtained from the following sources: Lu(1972) • ; Selmes and Tritton(1975) ■ ; McGimsey et al. (1975) × ; This paper △ . Visvanathan(1973) o Pomphrey et al.(1976) ρ

Figure 2. The radio spectrum of 3C454.3 between 10 MHz and 100 GHz for early 1972. The spectral decomposition is by eye-estimate although guided by our VLBI results for April 1972. Total flux density data were taken from the following sources:

38MHz,178 MHz,750 MHz, Kellerman et al.(1969)

53 MHz Harris (1974)

80 MHz Slee and Higgins(1973)

370 MHz Cotton (1975)

1400 MHz Roberts et al. (1975)

1667 MHz Shafer and Schilizzi (1975)

2700 MHz Altschuler and Wardle (1976)

5000 MHz Roberts et al.(1975)

7800 MHz This paper

8900 MHz Roberts et al.(1975)

15500 MHz Dent,Kapitzky and Kajoian (1974)

31400 MHz Dent and Hobbs(1973)

90000 MHz Fogarty et al.(1971)

Figure 3. The longest u-v tracks observed for each of the six interferometers. Units of u and v are millions of wavelengths. Tic marks are one hour apart. Locations which allow maxima and minima are enclosed by ellipses and rectangles, respectively. The principle maximum found from the earlier data is labelled $M_o(E)$. The principle maximum found from the 1974 May and 1974 October Haystack-NRAO data is labelled $M_o(L)$.

Figure 4. Correlated flux and clcsure phase data for3C454.3. The dates of the experiments and antenna pairs used are given next to the corresponding data. For closure phase, the data and model predictions for each combination are denoted by the following symbols and lines, except that the single NGS closure phase predicted value for each of the 1973 August and 1973 October experiments is indicated by ···.

HNG=• = ————

HNS=× =--------

HGS=□ =—·—·—·—·

NGS=△ =··········

Figure 5. Contour diagrams for the models presented in Table II. Tic marks are every millarcsecond and the contour level spacing is 2Jy/milliarcsecond^2 with the first level at .25. Components 1-4 are labelled on the 1974 May model.

Figure 6. Polarized flux spectrum of 3C454.3. Data were taken from the following sources:

365 MHz Conway et al.(1972)
610 MHz Conway et al.(1972)
960 MHz Haves et al.(1974)
1.4 GHz Gardner et la.(1969a) and Bologna et al.(1969)
1.7 GHz Berge and Seilstad(1967)
2.7 GHz Altschuler and Wardle(1976) and Gardner el al.(1969a)
4.1 GHz Tabara et al. (1972)
5.0 GHz Ryle et al. (1975) and Gardner et al.(1969b)
6.6 GHz Bignell and Seaquist (1973)
8.0 GHz Altschuler and Wardle (1976)
10.7 GHz Bignell and Seaquist(1973)
19.5 GHz McCullough and Waak (1969)
31.4 GHz Hobbs and Waak (1972)

Figure 7. Total flux variations at 2.7GHz, 7.8 GHz,15.5 GHz and 31.4 GHz. Outbursts labelled A,B and C are referred to in the text. A dashed line has been drawn through the six data points at 41.4 GHz to suggest outbursts A and B. Data were taken from the following sources:

2.7 GHz Altschuler and Wardle (1976)
7.8 GHz ○ This paper
7.8 GHz • Altschuler and Wardle (1976)
7.8 GHz × Dent and Kajoian (1972) and Dent (private communication.)
15.5 GHz Dent, Kapitzky and Kajoizn (1974)
31.4 GHz Dent and Hobbs (1973)

Figure 8. Theoretical flux densities of component 2 as a function of the relative radius parameter $\rho = r/r_o$, based on van der Laan's theory. The curves were generated using equation VI.3 with ν_m = 9GHz, S_{mo}=10.5 Jy and τ_m =.26. The maximum flux density at 31.4 GHz, not shown, is ~70 Jy and occurs near ρ =.4.

Figure 9. 3C454.3 outburst during 1971-1973 at 2.7,7.8,15.5 and 31.4 GHz with two background components subtracted off. Dashed line is the least-squares fit of peaked injection model. Model parameters and their 1-σ formal errors are as follows: a=.019$\pm$.004;b=8.8x10$^3\pm$2.5x10^3; ρ =1.05$\pm$.11; γ =1.1$\pm$.04; ϵ =.55$\pm$.034; δ =1.5, t_o=1971.0.

Figure 10 3C454.3 outburst during 1965-1969 at 2.7,6.6,7.8,10.7 and 31.4 GHz. Data were taken from the following sources: 2.7 GHz,Witzel and Veron(1971);6.6GHz and 10.7 GHz, Medd et al(1972); 7.8 GHz Dent and Kajoian (1972); 31.4 GHz,McCullough and Waak (1972). Dashed line is the least-squares fit of peaked injection model after the halo background component was subtracted off. Model parameters and their 1-σ formal errors are as follows: a=.012$\pm$.0005;b=8.6x10$^3\pm$.48x10^3; ρ fixed at .6; γ =2.36$\pm$.03; ϵ =.72$\pm$.03. δ =1.7,t_o=1965.2.

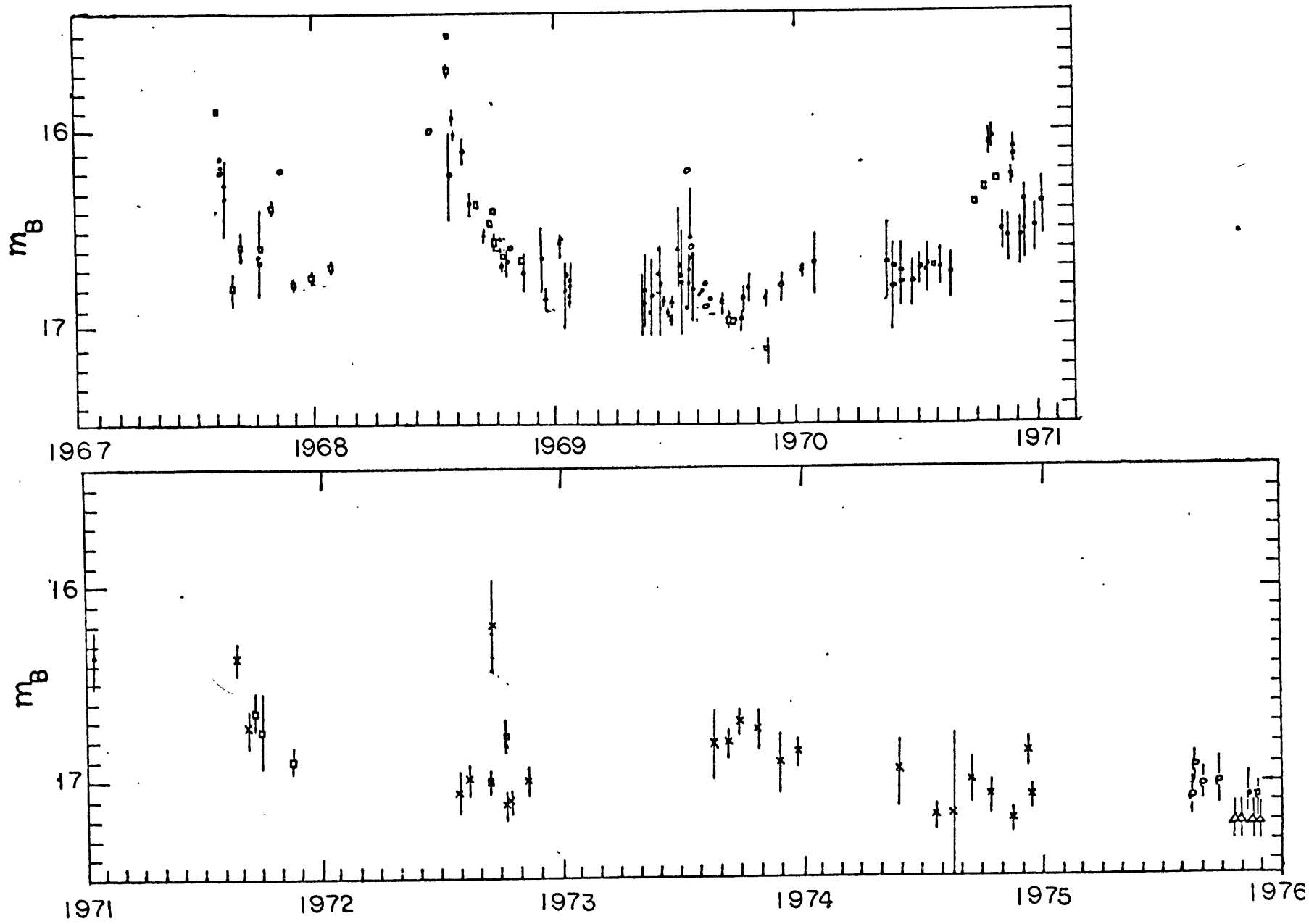
16
17
m_B
1967
1968
1969
1970
1971
16
17
m_B
1971
1972
1973
1974
1975
1976

FIGURE 1

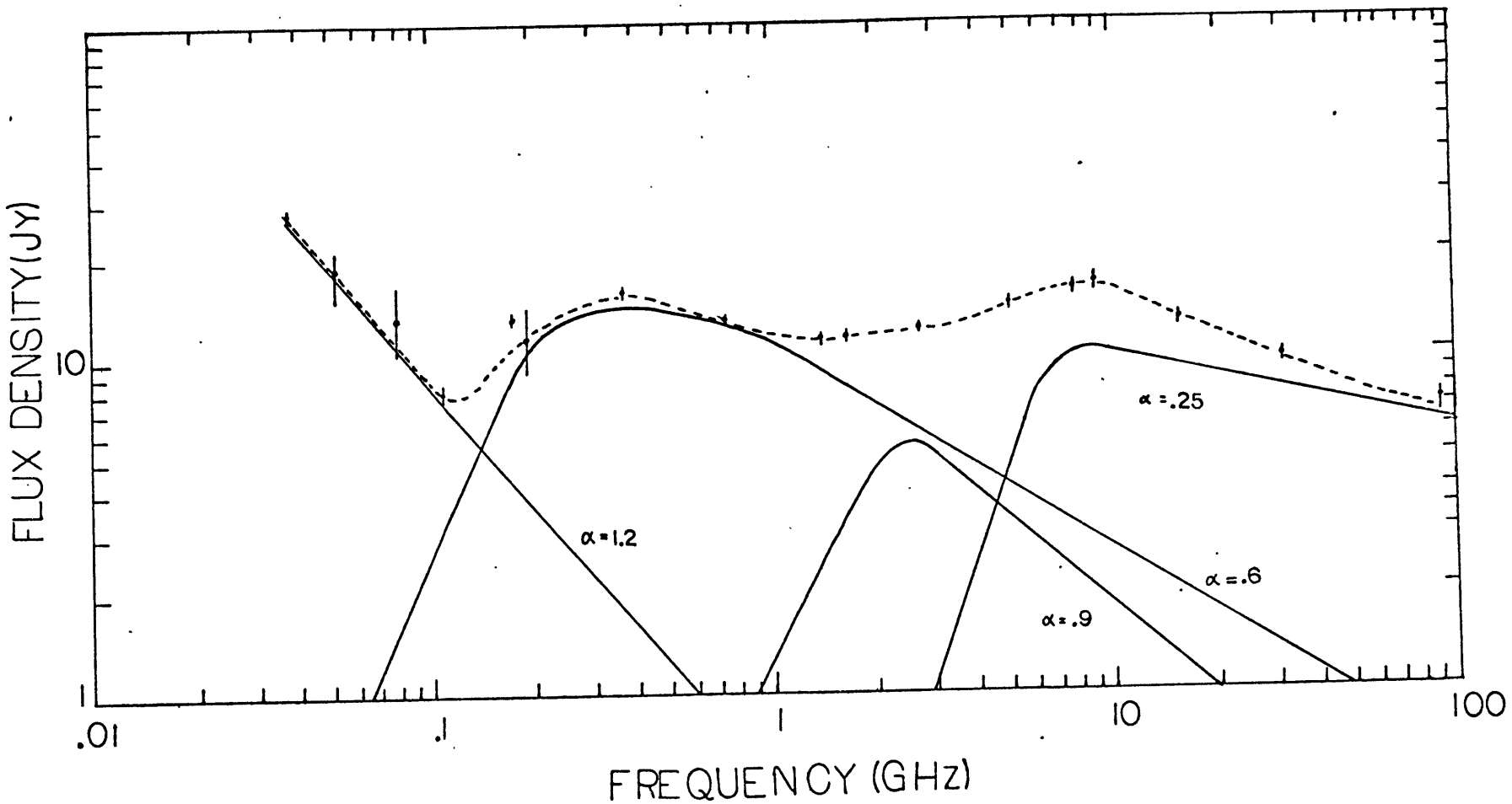

FIGURE 2

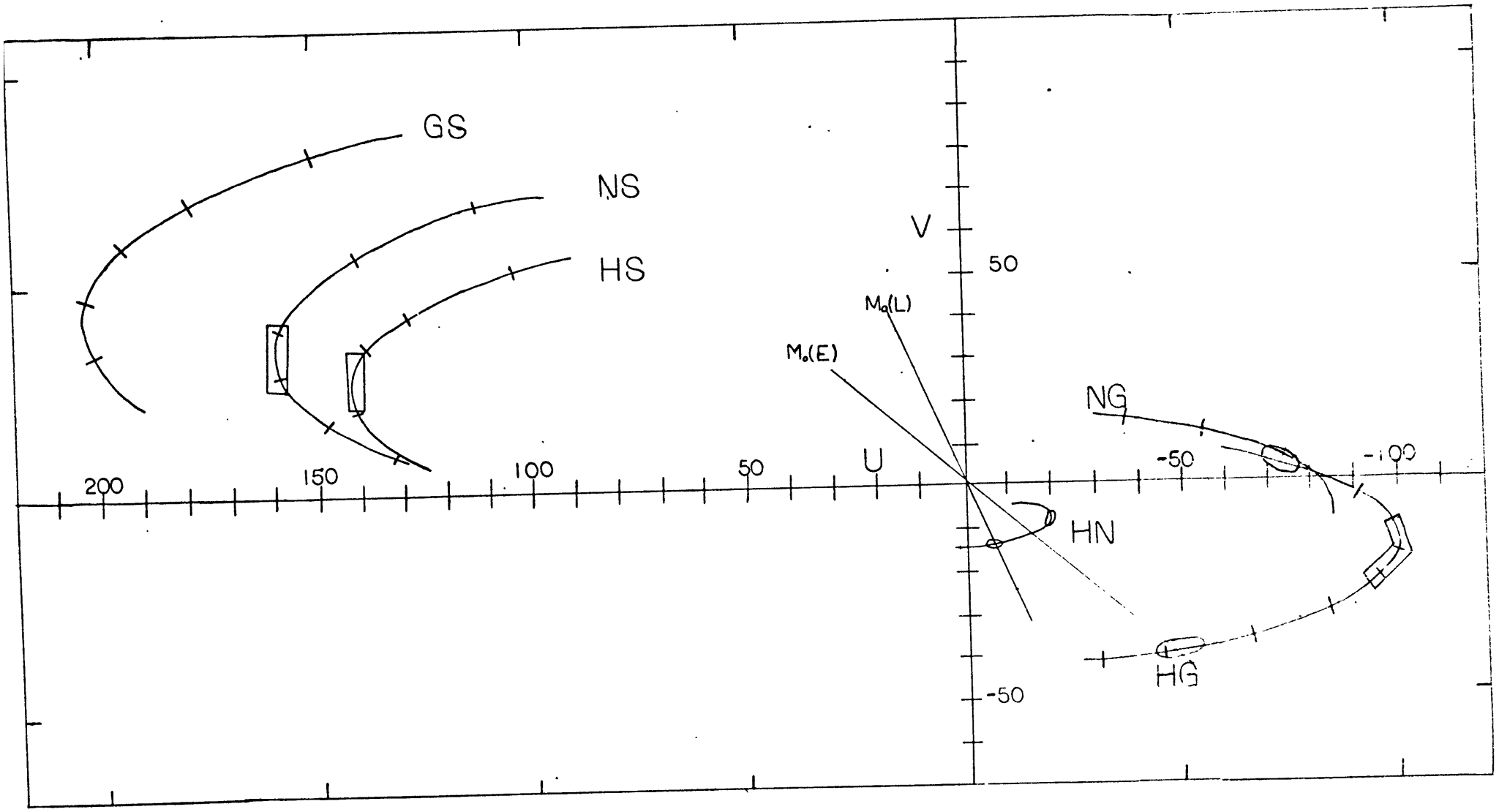

FIGURE 3

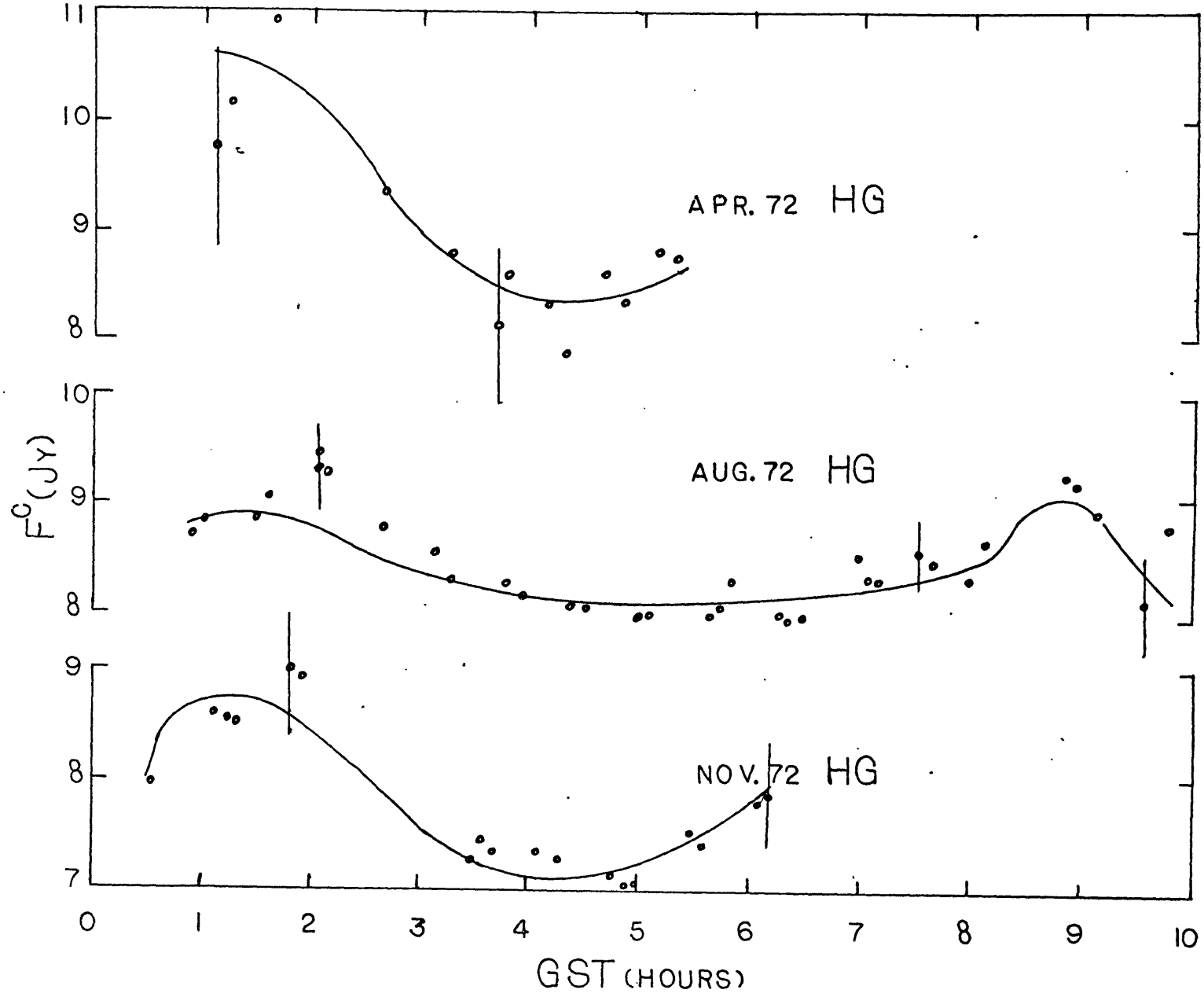

FIGURE 4

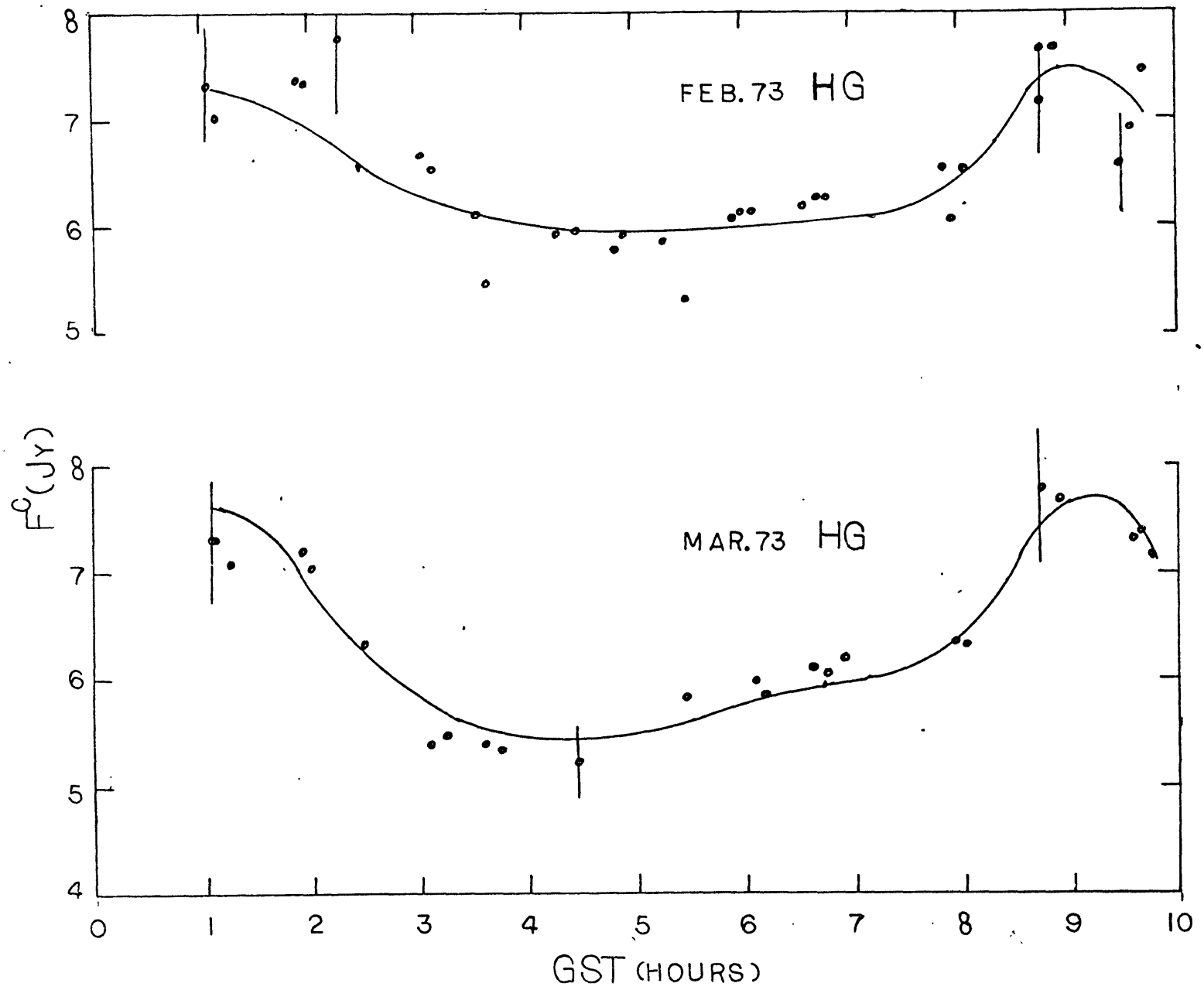

FIGURE 4

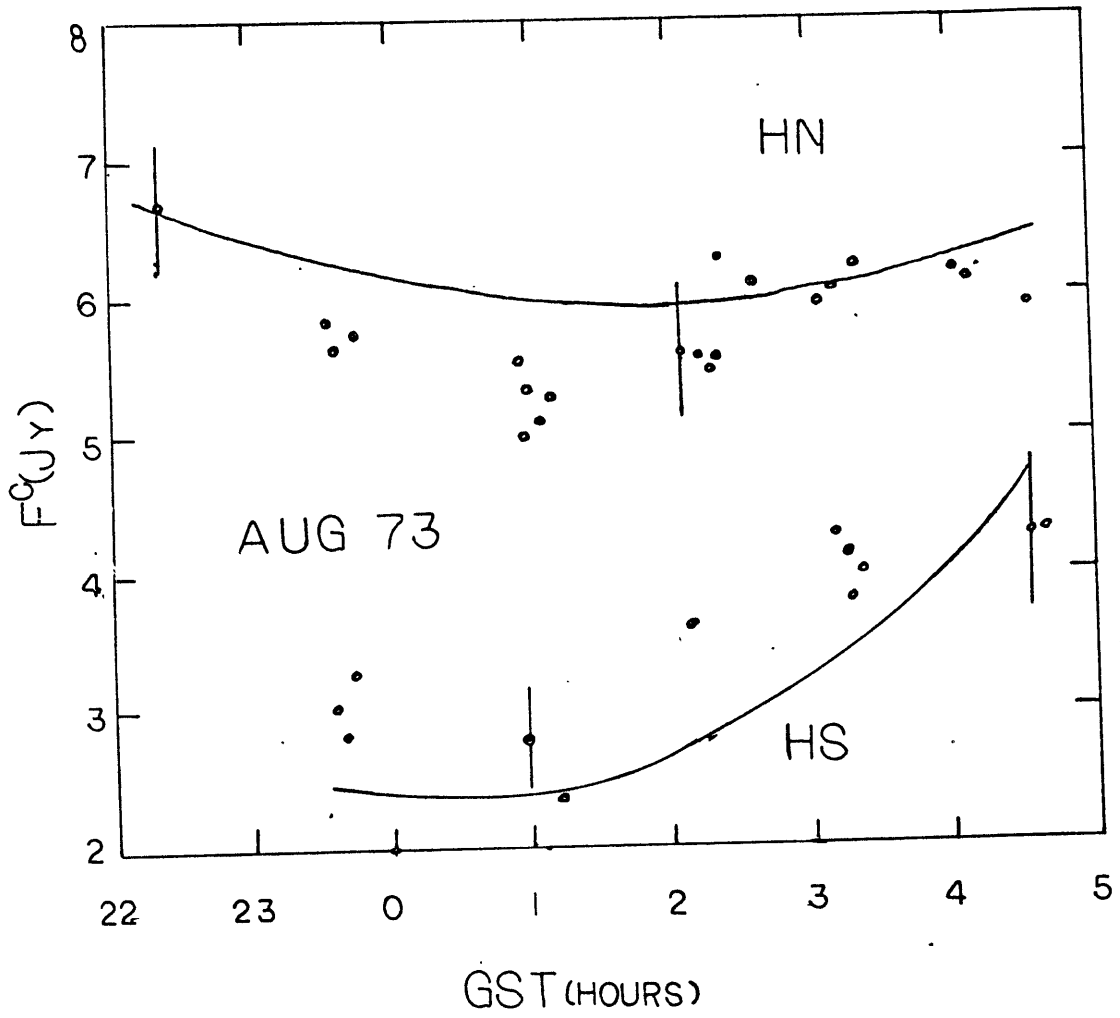

FIGURE 4

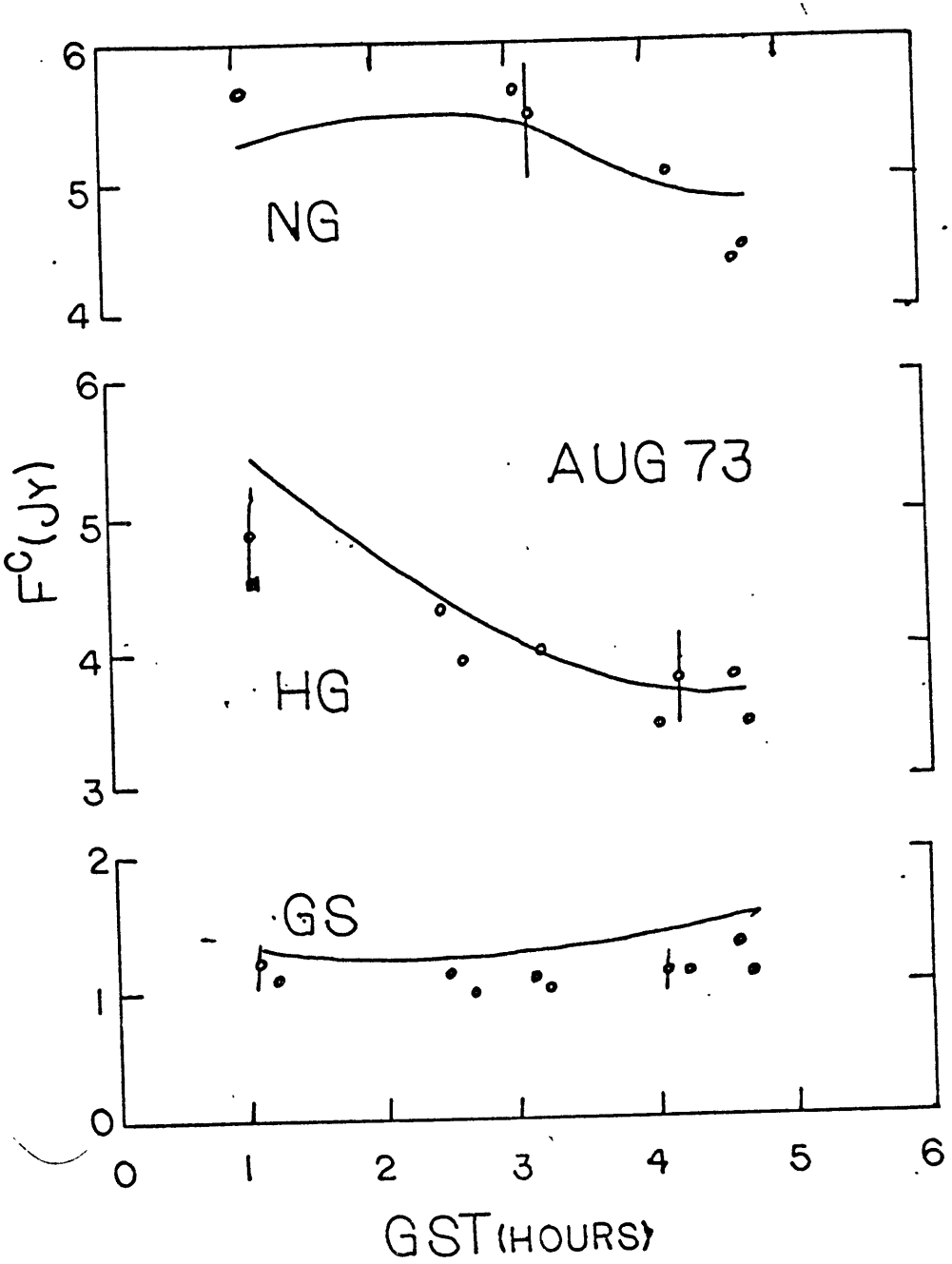

FIGURE 4-

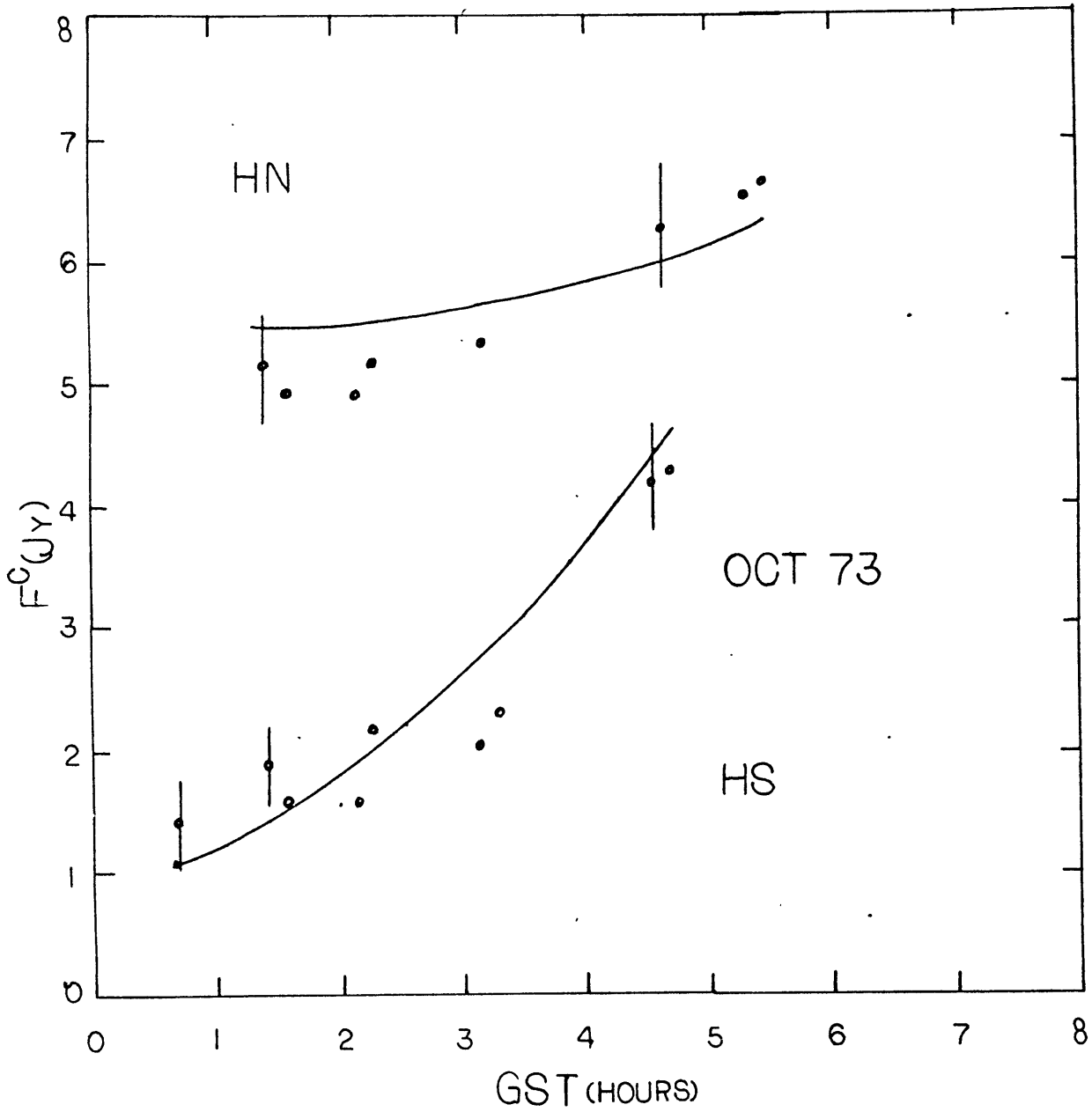

FIGURE 4

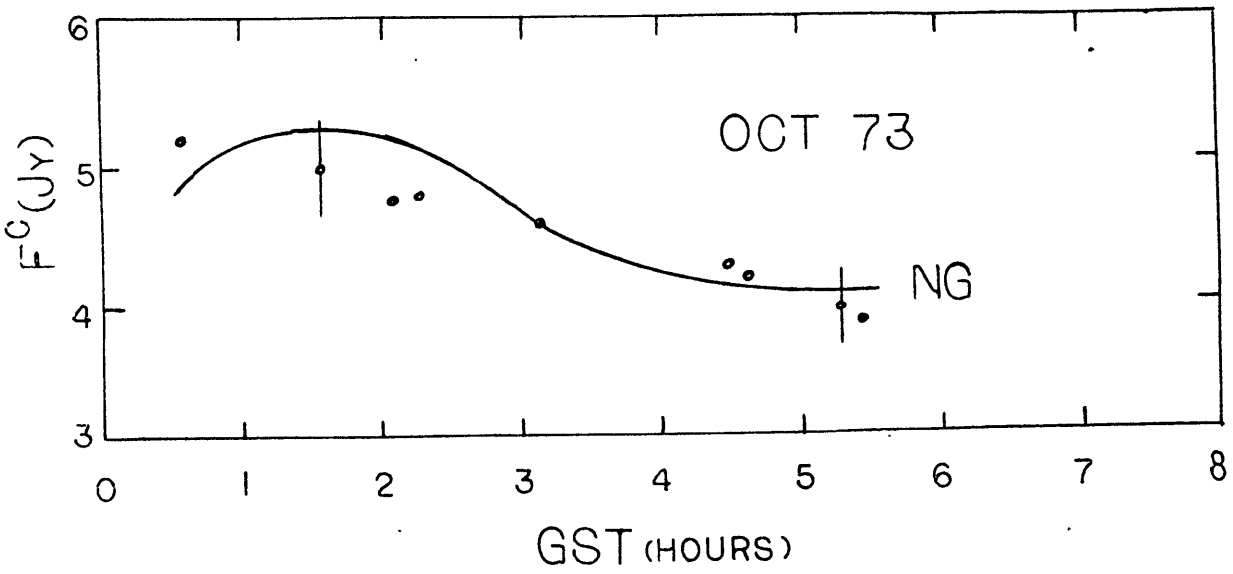

FIGURE 4

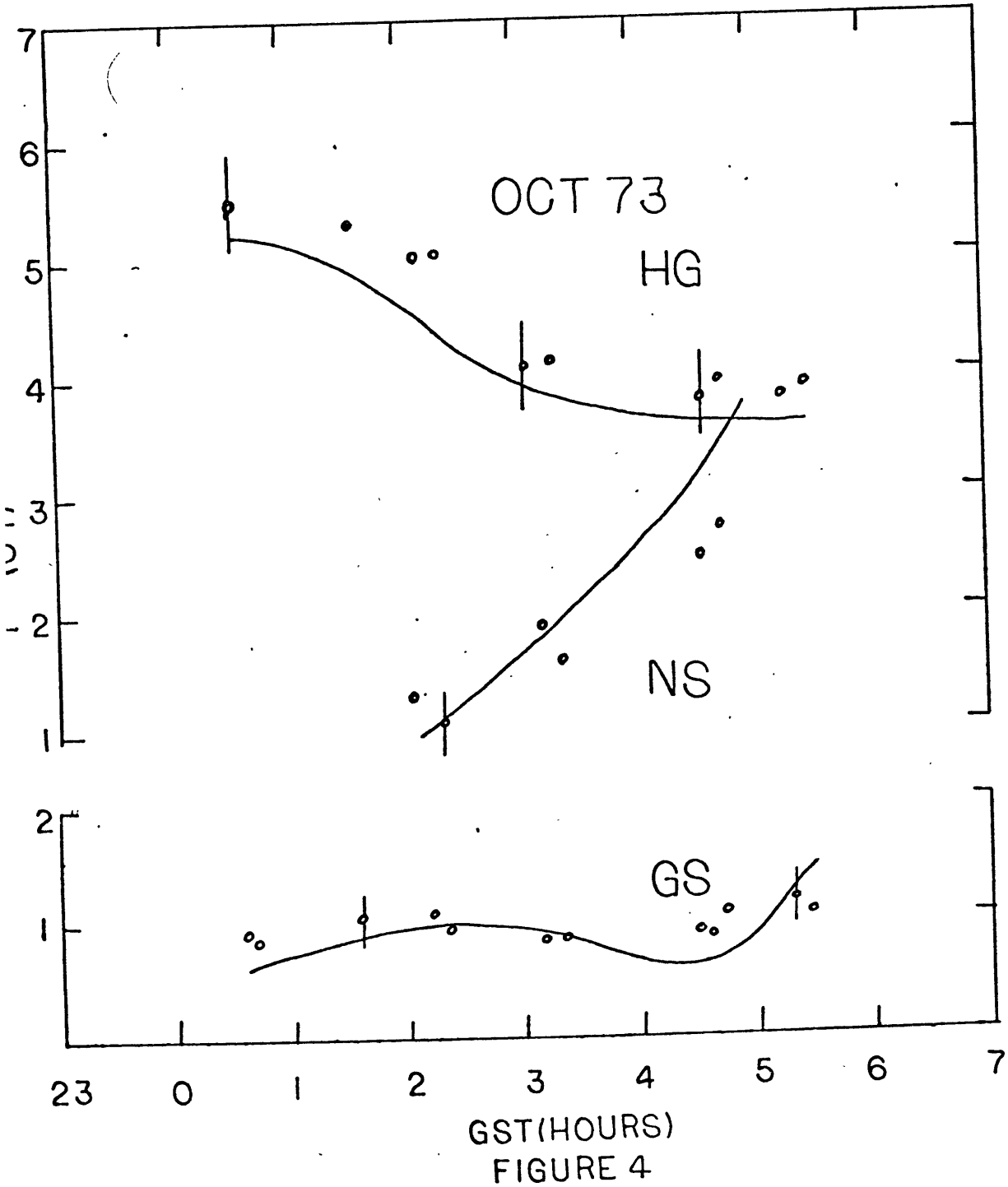

FIGURE 4

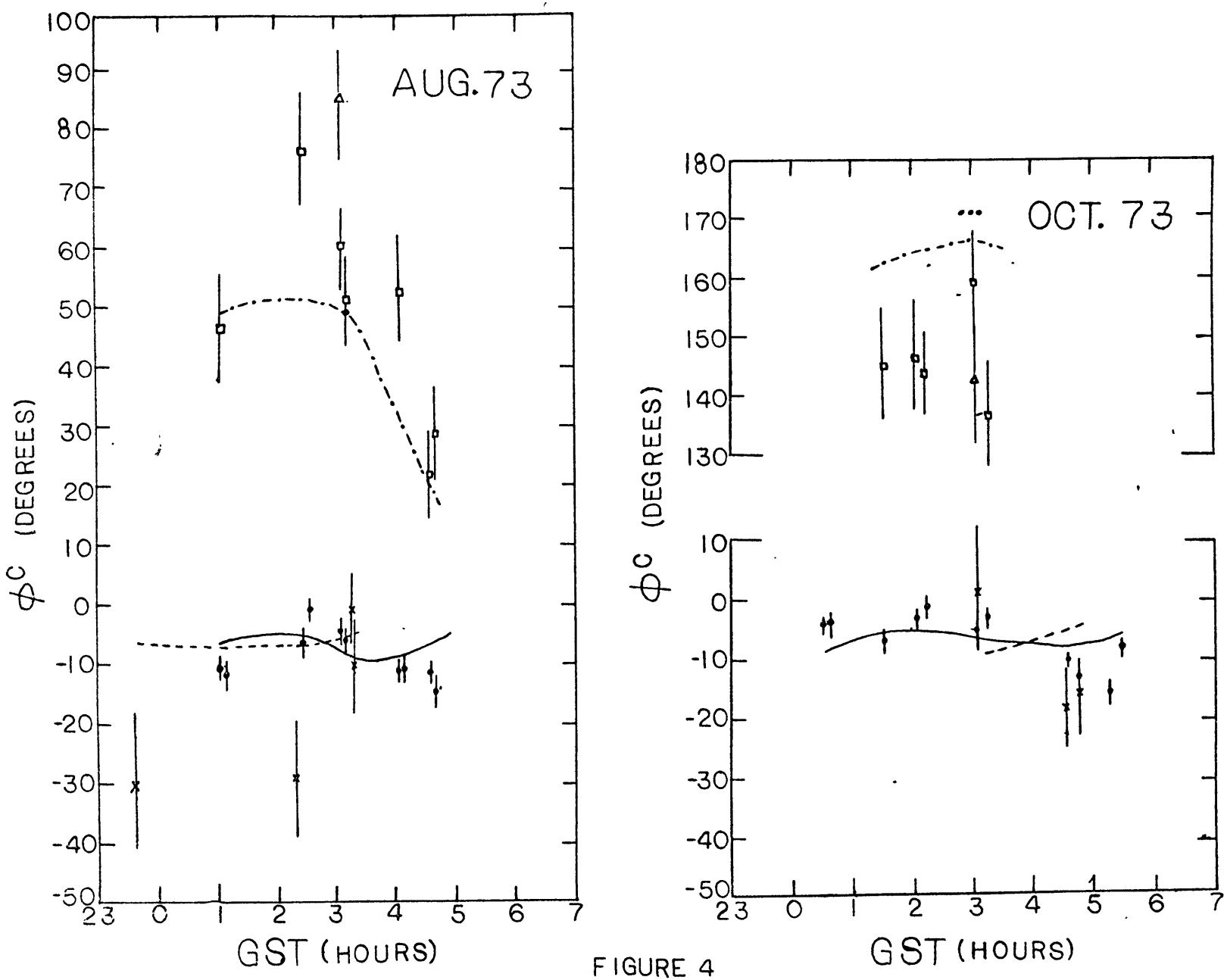
AUG.73
OCT. 73
ϕ^C (DEGREES)
GST (HOURS)
100
90
80
70
60
50
40
30
20
10
0
-10
-20
-30
-40
-50
180
170
160
150
140
130
23
0
1
2
3
4
5
6
7

FIGURE 4

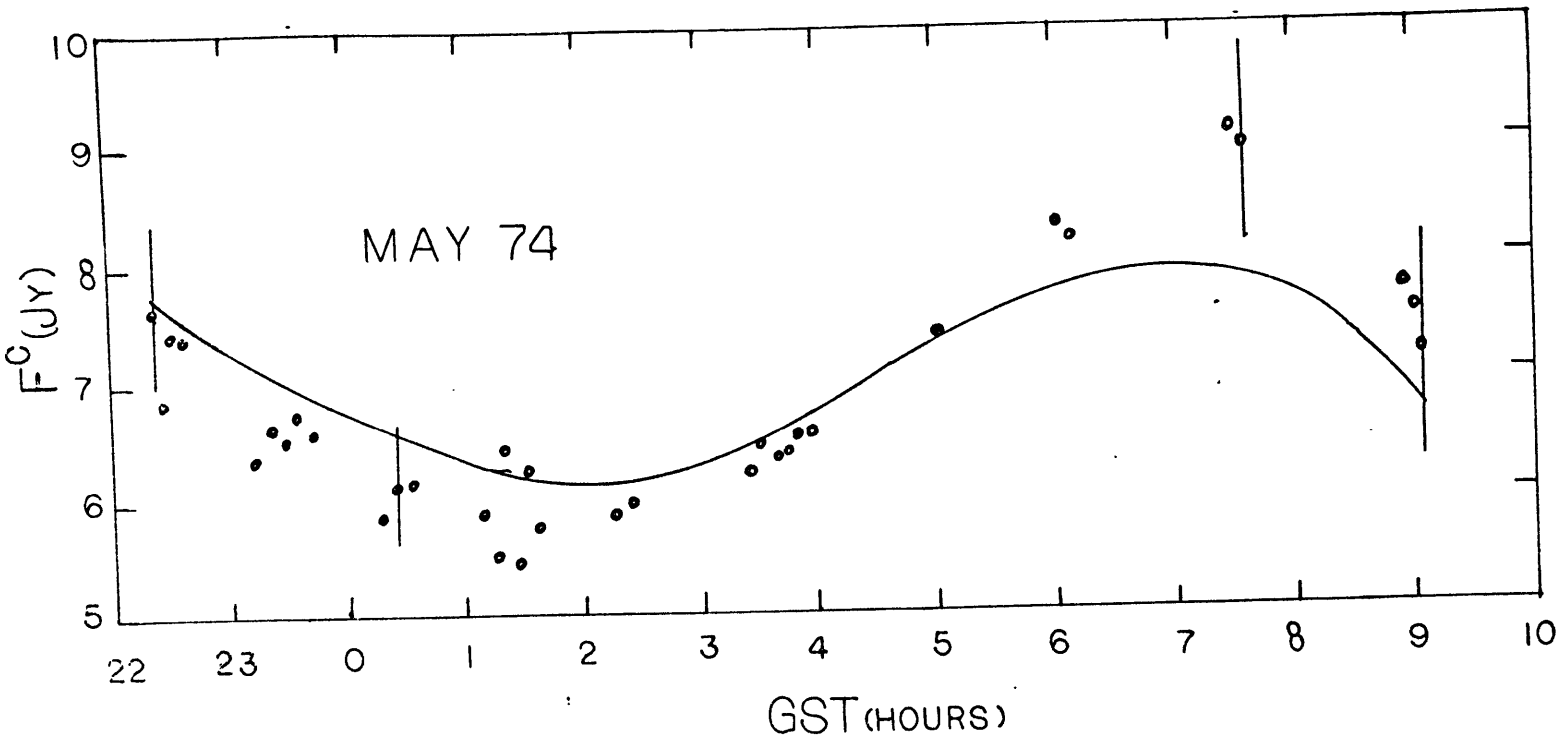

FIGURE 4

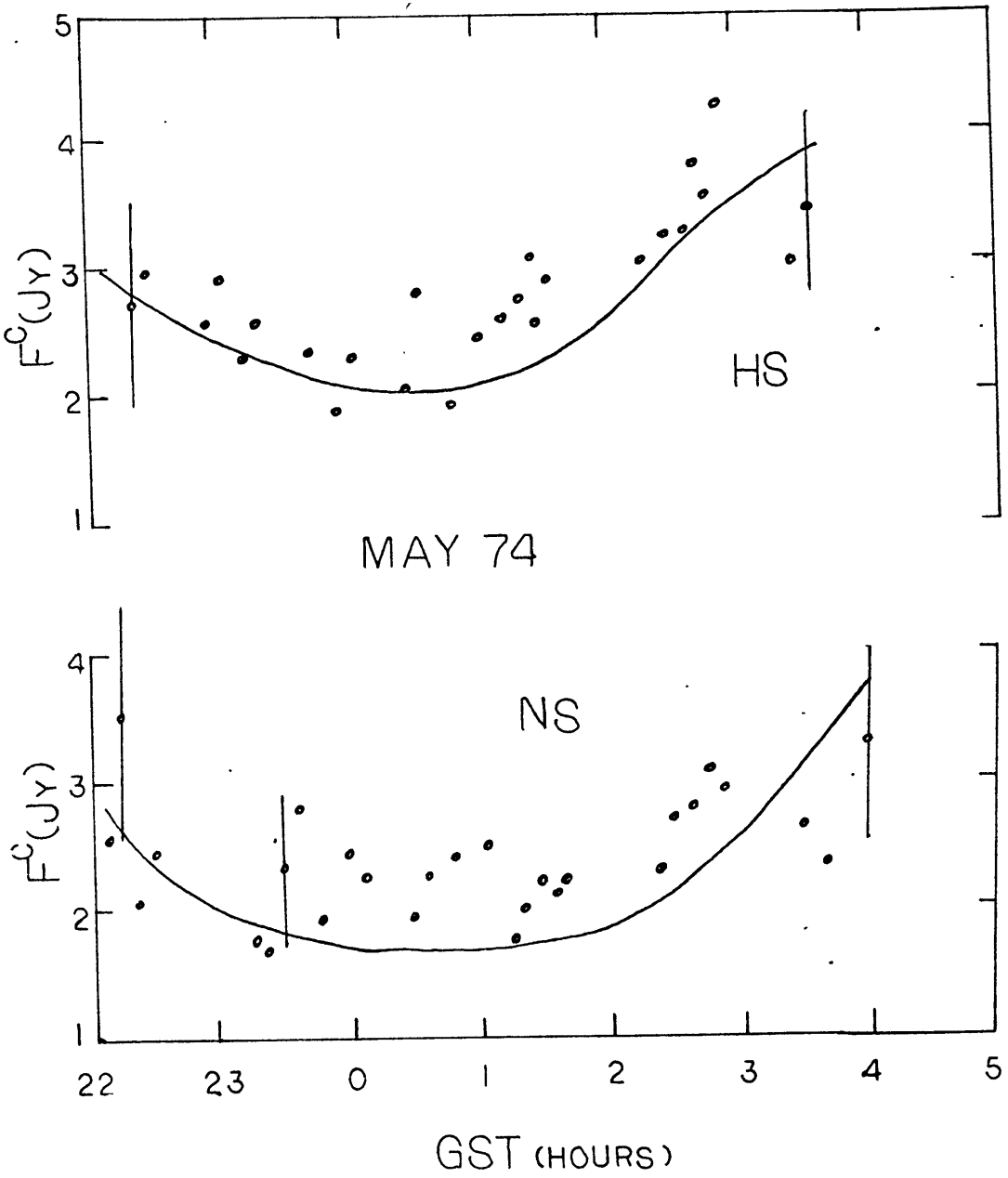

FIGURE 4

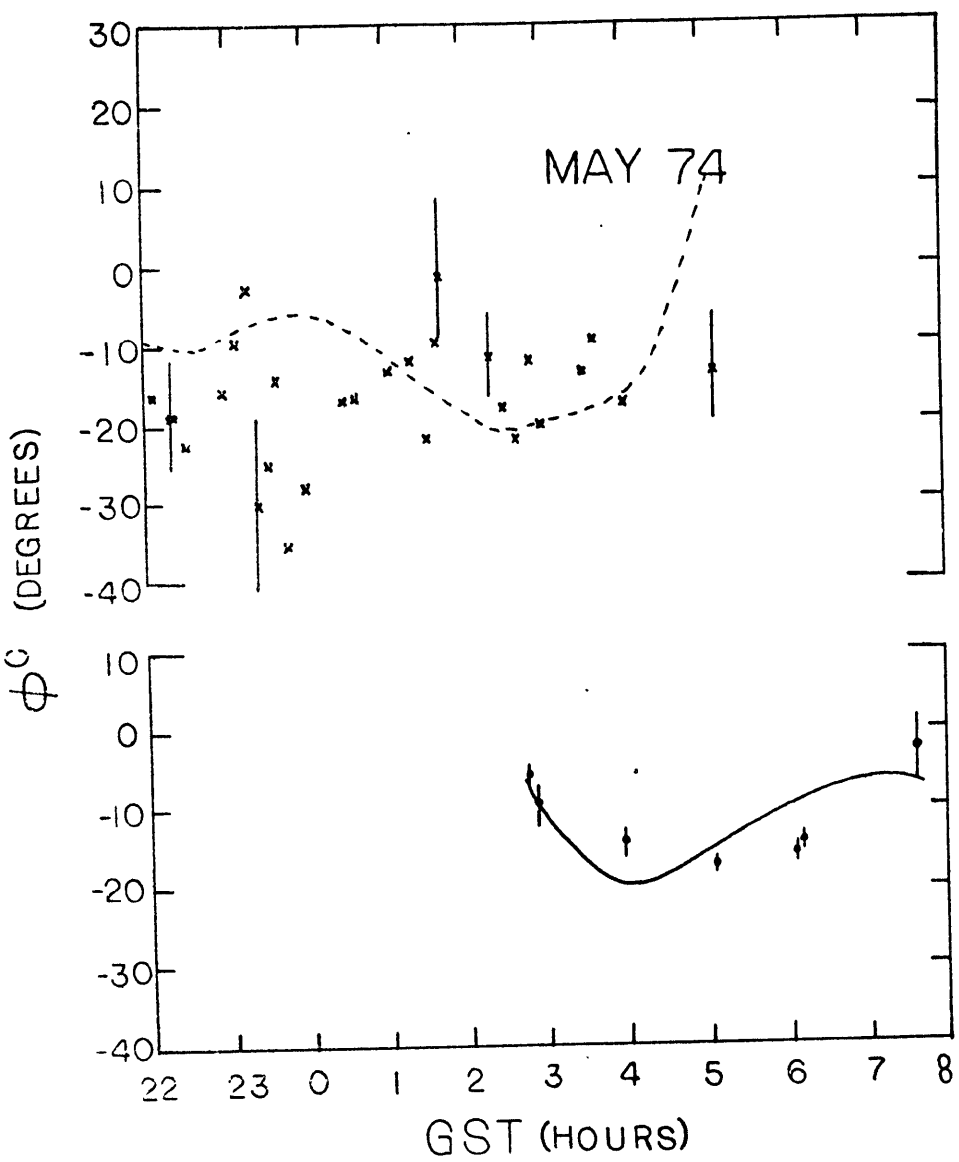
MAY 74
30
20
10
0
-10
-20
-30
-40
10
0
-10
-20
-30
-40
22
23
0
1
2
3
4
5
6
7
8
GST (HOURS)
ϕ^C (DEGREES)

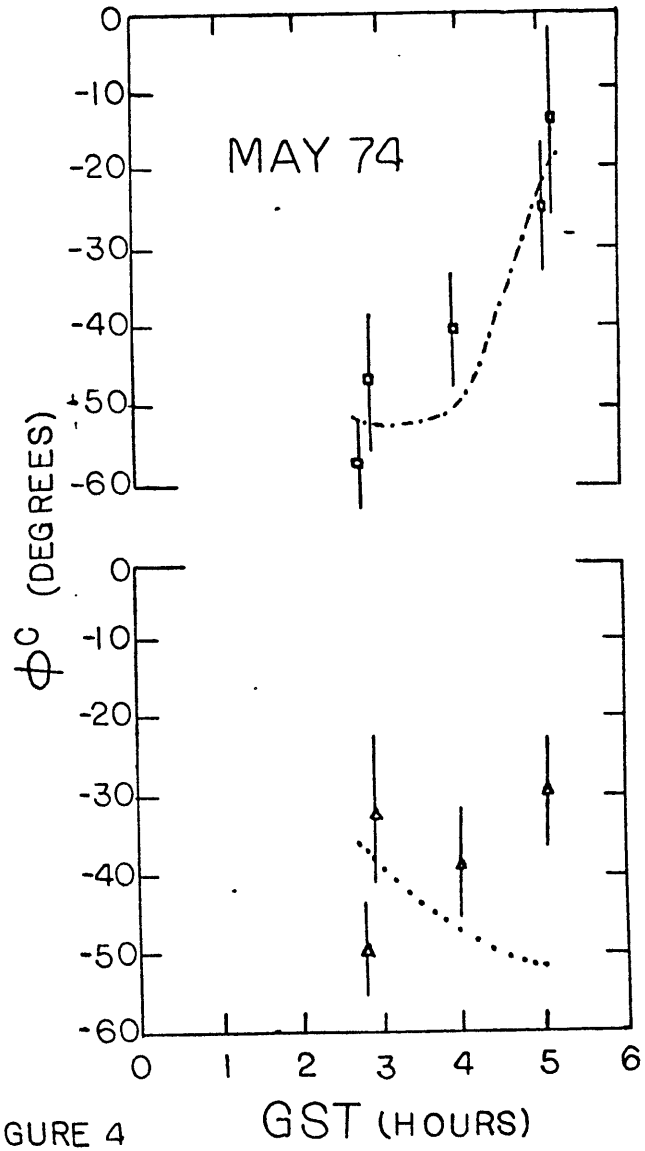
MAY 74
0
-10
-20
-30
-40
-50
-60
0
-10
-20
-30
-40
-50
-60
0
1
2
3
4
5
6
GST (HOURS)
ϕ^C (DEGREES)

FIGURE 4

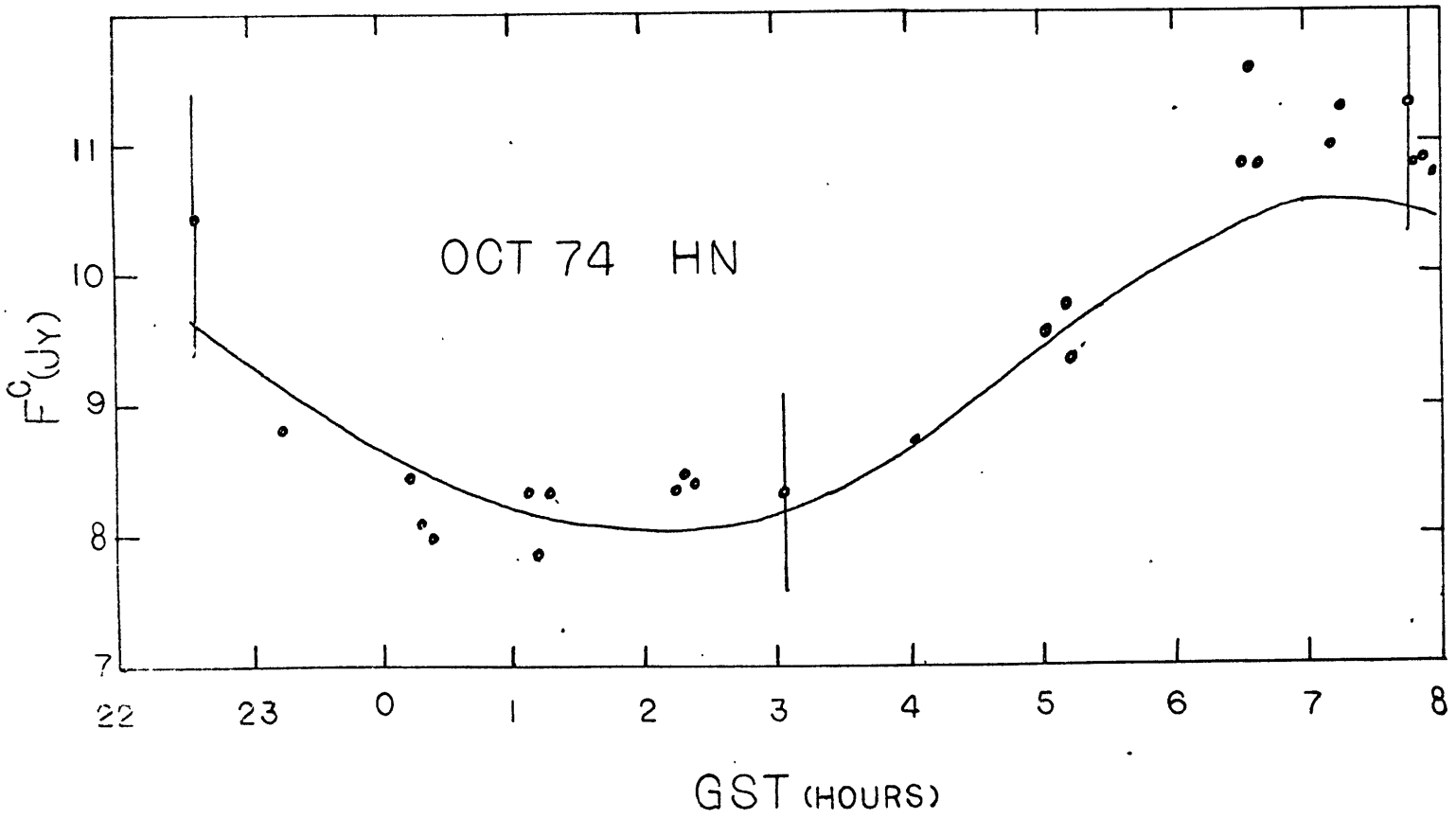

FIGURE 4

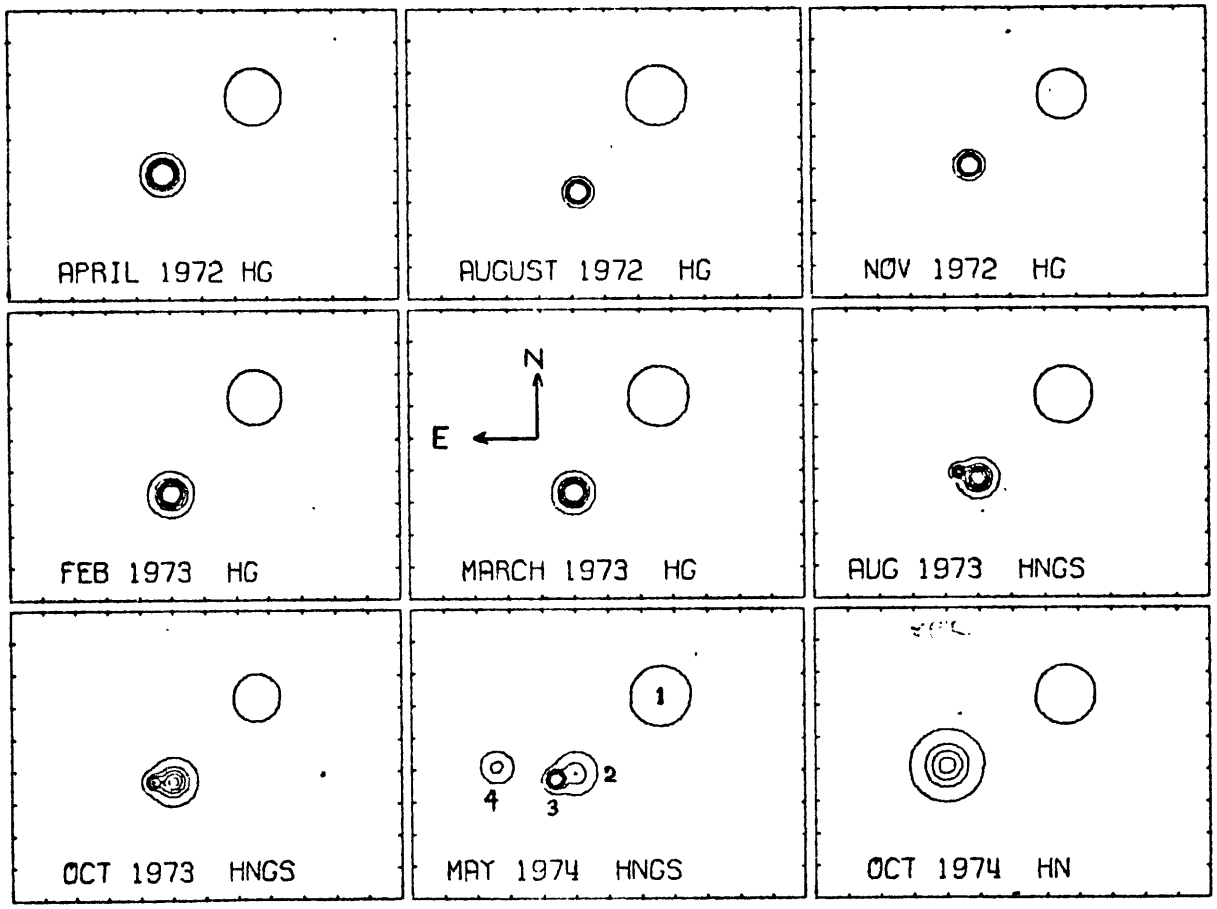
APRIL 1972 HG
AUGUST 1972 HG
NOV 1972 HG
FEB 1973 HG
N
E
MARCH 1973 HG
AUG 1973 HNGS
OCT 1973 HNGS
1
2
3
4
MAY 1974 HNGS
OCT 1974 HN

FIGURE 5

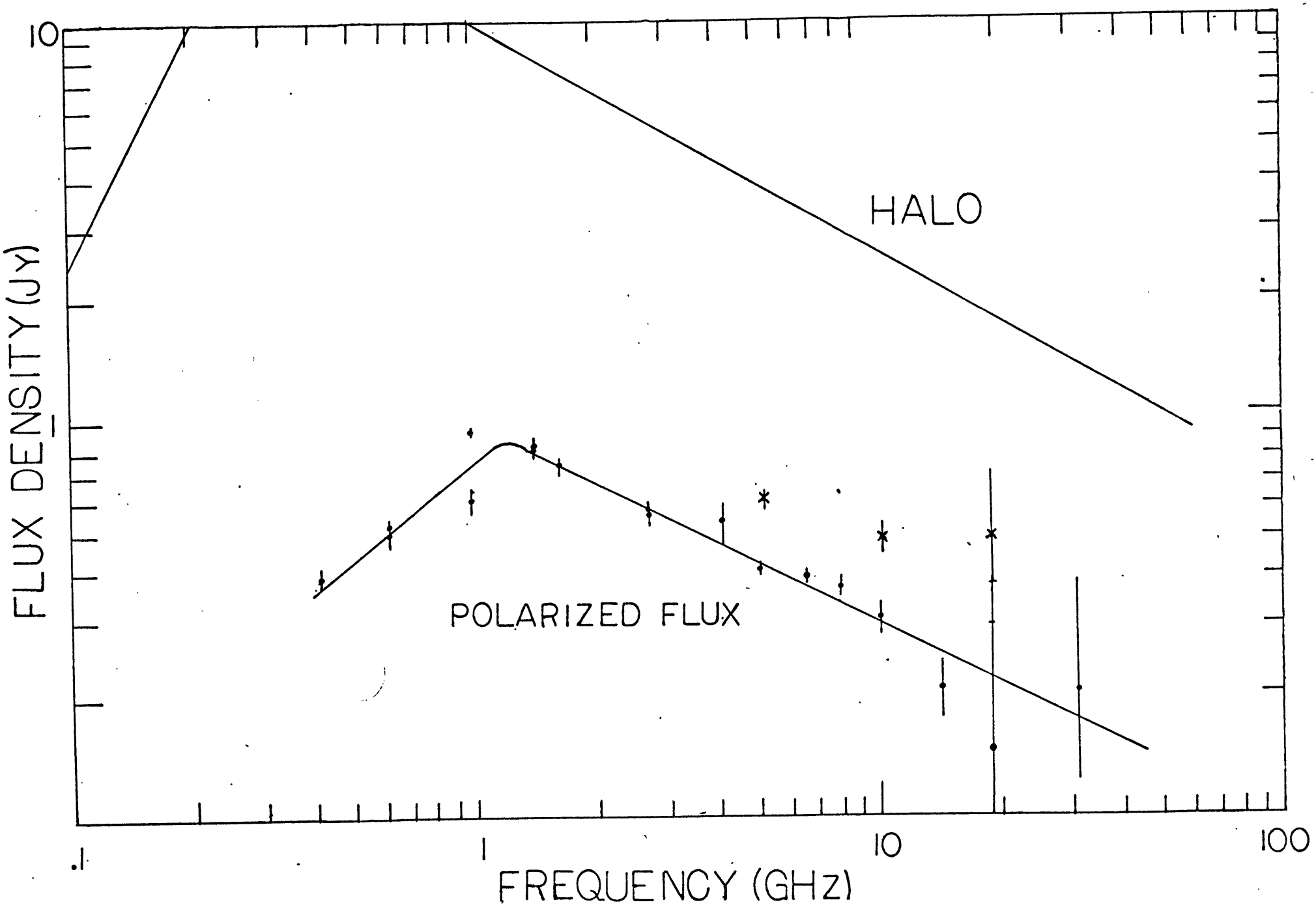
10
FLUX DENSITY (JY)
HALO
POLARIZED FLUX
.1
1
10
100
FREQUENCY (GHz)

FIGURE 6

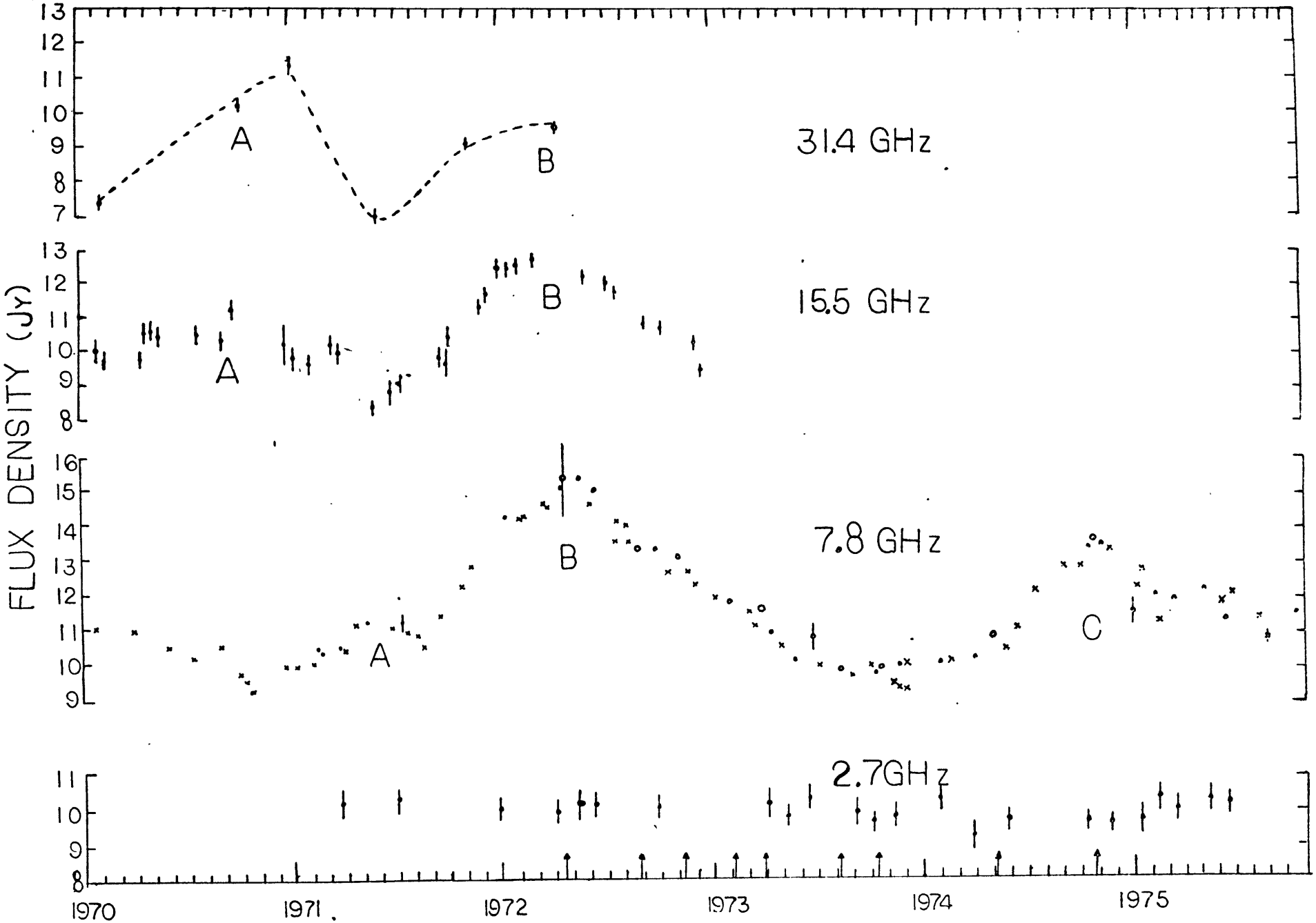
FLUX DENSITY (JY)
31.4 GHz
15.5 GHz
7.8 GHz
2.7GHz
A
B
C
1970
1971
1972
1973
1974
1975

FIGURE 7

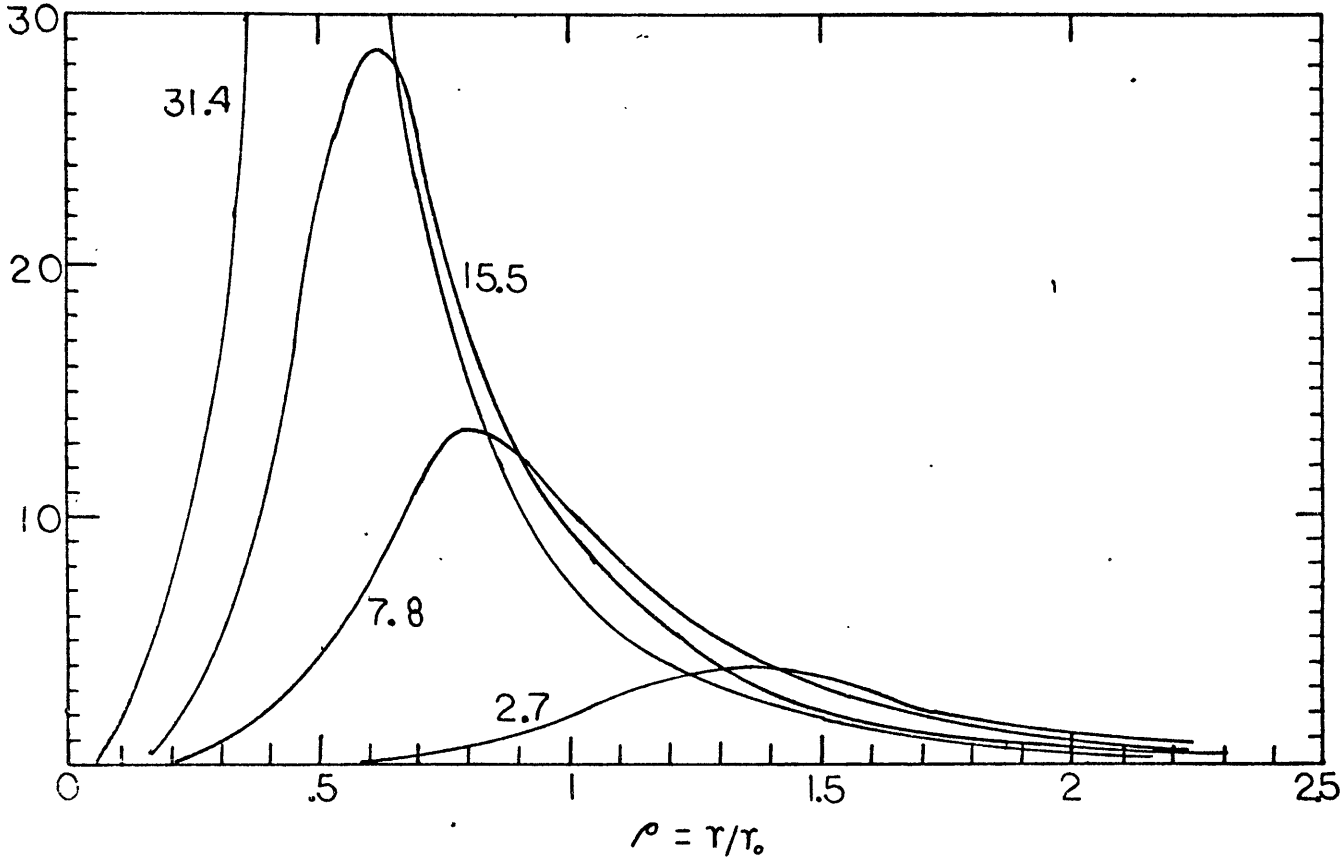

FIGURE 8

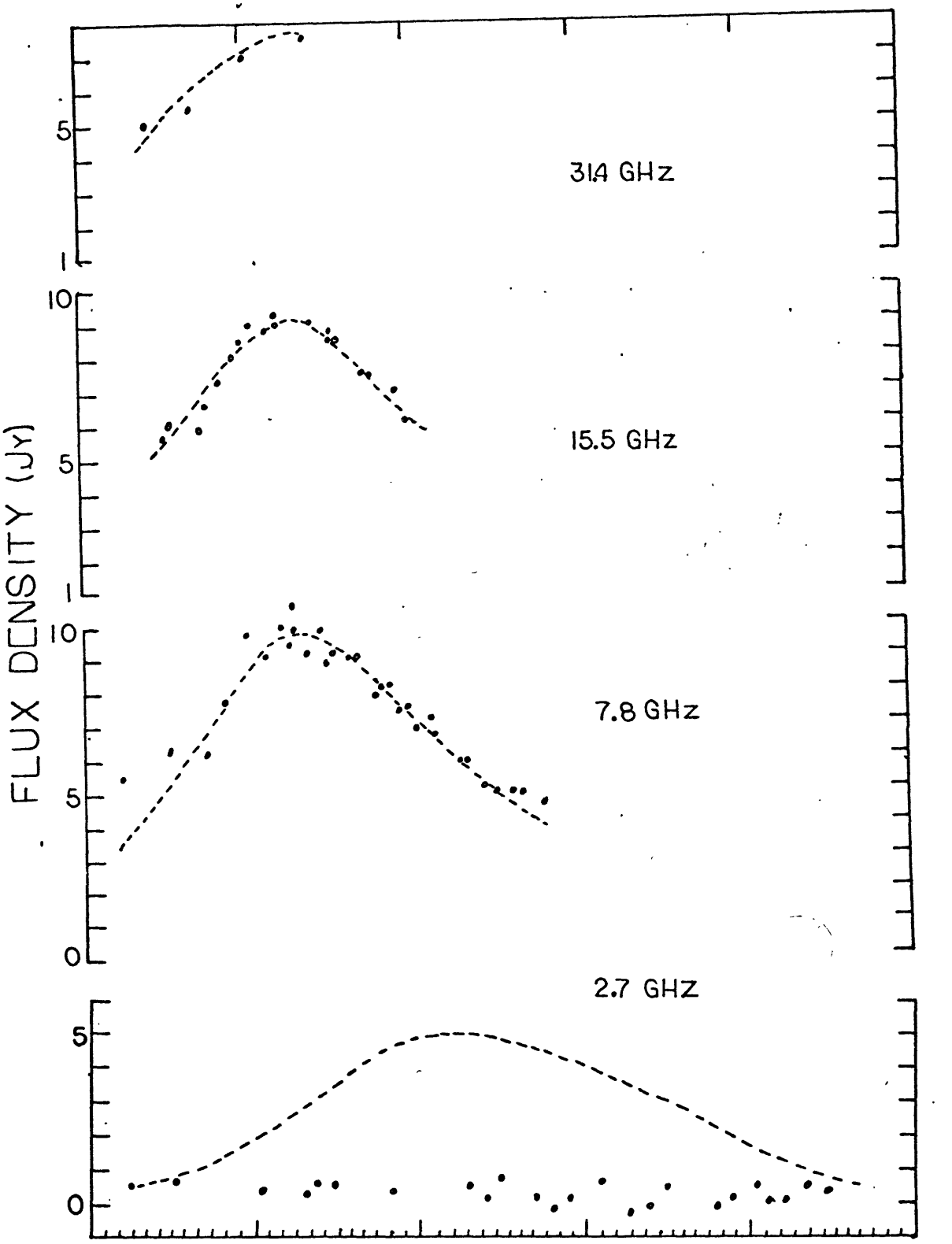
FLUX DENSITY (JY)
31.4 GHz
15.5 GHz
7.8 GHz
2.7 GHZ
10
5
1
10
5
0
5
0
1971
1972
1973
1974
1975
1976

FIGURE 9

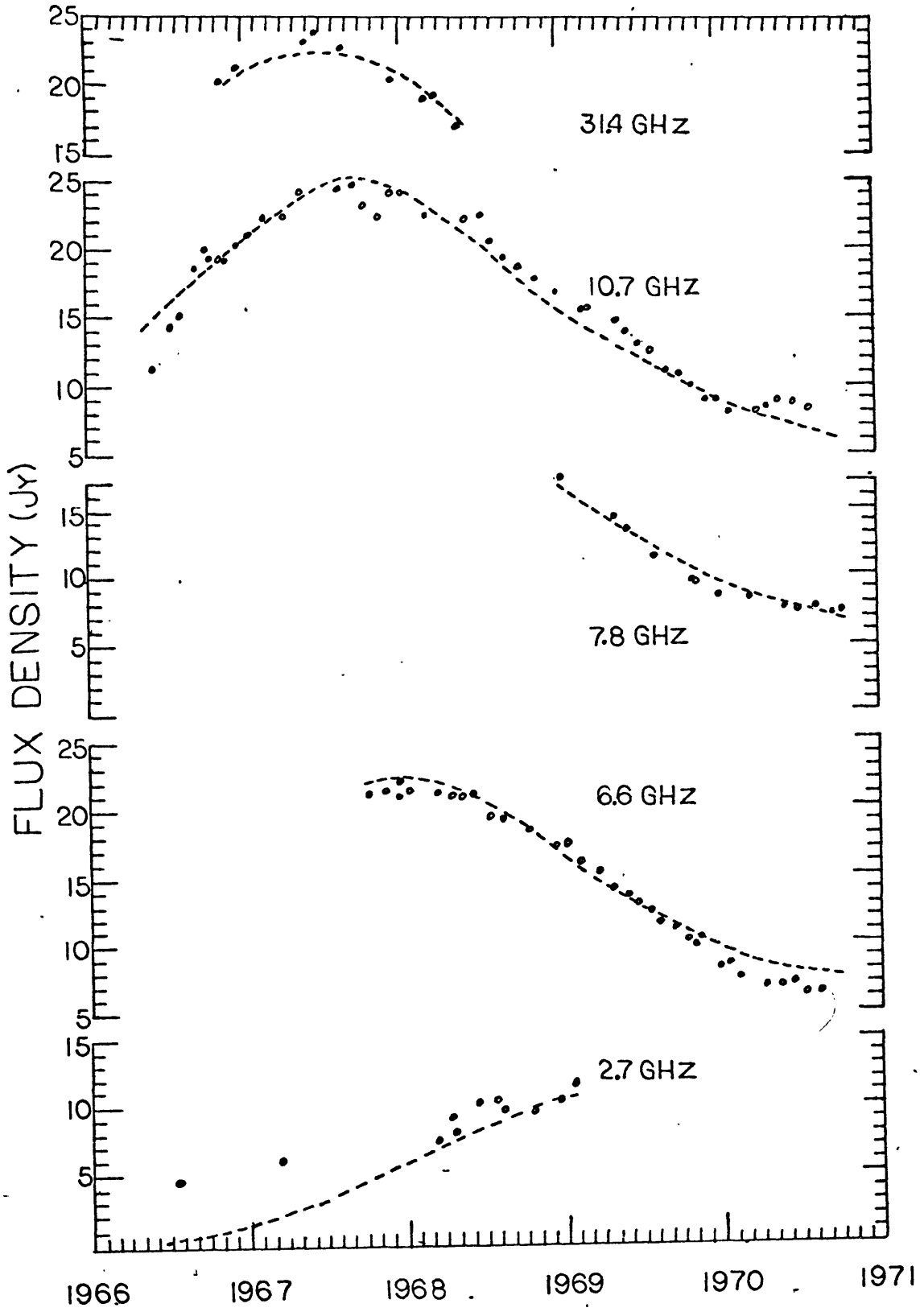
FLUX DENSITY (JY)
25
20
15
3.14 GHz
25
20
15
10
5
10.7 GHz
15
10
5
7.8 GHz
25
20
15
10
5
6.6 GHz
15
10
5
2.7 GHz
1966
1967
1968
1969
1970
1971

FIGURE 10